Mineralogy and Petrology (2018) 112 (Suppl 1):S23–S41
https://doi.org/10.1007/s00710-018-0577-8

ORIGINAL PAPER

The birth, growth and ageing of the Kaapvaal subcratonic mantle

Gerhard P. Brey[1] · Qiao Shu[2,3]

Received: 13 December 2017 / Accepted: 20 April 2018 / Published online: 1 June 2018

Abstract

The Kaapvaal craton and its underlying mantle is probably one of the best studied Archean entity in the world. Despite that, discussion is still vivid on important aspects. A major debate over the last few decades is the depth of melting that generated the mantle nuclei of cratons. Our new evaluation of melting parameters in peridotite residues shows that the Cr_2O_3/Al_2O_3 ratio is the most useful pressure sensitive melting barometer. It irrevocably constrains the pressure of melting (melt separation) to less than 2 GPa with olivine (ol), orthopyroxene (opx) and spinel (sp) as residual phases. Garnet (grt) grows at increasing pressure during lithosphere thickening and subduction via the reaction opx + sp → grt + ol. The time of partial melting is constrained by Re-depletion model ages (T_{RD}) mainly to the Archean (Pearson and Wittig 2008). However, only 3% of the ages are older than 3.1 Ga while crustal ages lie mainly between 3.1 to 2.8 Ga for the W- and 3.7 to 2.8 Ga for the E-block. Many T_{RD}-ages are probably falsified by metasomatism and the main partial melting period was older than 3.1 Ga. Also, Nd- and Hf- model ages of peridotitic lithologies from the W-block are 3.2 to 3.6 Ga old. The corresponding very negative εNd (−40) and εHf values (−65) signal the presence of subducted crustal components in these old mantle portions. Subducted components diversify the mantle in its chemistry and thermal structure. Adjustment towards a stable configuration occurs by fluid transfer, metasomatism, partial melting and heat transfer. Ages of metasomatism from the Lu-Hf isotope system are 3.2 Ga (Lace), 2.9 Ga (Roberts Victor) and 2.62 Ga (Finsch) coinciding with the collision of cratonic blocks, the growth of diamonds, metamorphism of eclogites and of Ventersdoorp magmatism. The cratonic lithosphere was stabilized thermally by the end of the Archean and cooled since then with a rate of 0.07 °C/Ma.

Keywords Subcratonic mantle · Metasomatism · Archean subduction · Cooling of the mantle · Cr/Al ratio as melting barometer

Introduction

The subcratonic mantle is the site for the storage of early products of partial melting and fractional crystallization of the Earth. It consists of two major components, volumetrically dominating ultramafic rocks (peridotites) and a subordinate mafic portion (eclogites and garnet pyroxenites). Partial melting, metamorphism and metasomatism imposed by tectonic forces and terminating thermal stabilization were the main processes that contributed to the birth, growth and ageing of the subcratonic lithospheric mantle. High to very high degrees of partial melting left a residuum with high Mg values (low Fe) and very low volatile contents (e.g. Walter 1998; Bernstein et al. 2007; Pearson and Wittig 2008; Peslier et al. 2010). The ensuing low density and the stiffness due to low OH led to buoyancy of the lithosphere that kept the crust at relatively constant height since the Archean (e.g. Jordan 1988; Peslier et al. 2010). Though there is a general acceptance that very high degrees of partial melting in the absence of garnet generated the residues, no consensus exists about the melting regime and the geodynamic setting in the Archean. Partial melting may have occurred at mid ocean

Editorial handling: G. Pearson

Electronic supplementary material The online version of this article (https://doi.org/10.1007/s00710-018-0577-8) contains supplementary material, which is available to authorized users.

✉ Gerhard P. Brey
brey@em.uni–frankfurt.de

[1] Institut für Geowissenschaften, Mineralogie, Goethe Universität Frankfurt, Altenhöferallee 1, D-60438 Frankfurt, Germany

[2] State Key Laboratory of Ore Deposit Geochemistry, Institute of Geochemistry, Chinese Academy of Sciences, Guiyang 550081, China

[3] Department of Earth and Atmospheric Sciences, University of Alberta, Edmonton, AB T6G 2E3, Canada

ridges followed by subduction similar to modern Earth (e.g. Helmstaedt and Schulze 1989) or by upwelling in a hotter Archean environment followed by down drag due to eclogitisation at the base of oceanic plateaus as another kind of subduction (e.g. Lee and Chin 2014). In opposition are models where the subcratonic mantle consists mainly of residual peridotite from plumes that were subcreted under a lithospheric lid (e.g. Boyd 1989; Griffin et al. 2009). In such models partial melting and melt separation occurred at pressures of more than 3 GPa followed by stationary cooling to generate the present day garnet peridotites.

An Archean age for partial melting and the birth of the Kaapvaal cratonic mantle has been clearly established with the Re-Os isotope system. A major peak of Rhenium depletion model ages at 2.7 Ga may reflect the main period of partial melting (e,g, Pearson and Wittig 2008). However, metasomatism is ubiquitous in the cratonic mantle and may have disguised older ages possibly dating back into the Paleoarchean. Ancient metasomatism was indicated by very negative εNd values in mantle samples (e.g. Menzies and Murthy 1980; Richardson et al. 1984) but defined ages were lacking before the work of Lazarov et al. (2009, 2012) and Shu et al. (2013). In the paper, we will discuss these ages further and use them as possible time markers for Re-metasomatism and the influence on the Re-Os isotope system and ensuing model ages. The subcratonic mantle finally stabilized and reached thermal equilibrium by the end of the Archean (Michaut and Jaupart 2007) and is ageing by slow cooling since then.

The geology of the crust

The E- and the W-block are the two main blocks of the Kaapvaal Craton (Fig. 1). The gneiss complexes in the Swaziland-Barberton area on the E-block constitute the oldest known crust formation with almost 3.7 Ga for a tonalitic gneiss (Schoene et al. 2008) while the earliest crustal rocks on the W-block are around 3.1 Ga old (Schmitz et al. 2004). The E-block consists of several fragments that amalgamated at around 3.2 Ga (Schoene et al. 2008). Both blocks evolved separately until they collided 2.88 Ga ago along the Colesberg lineament (Schmitz et al. 2004). Granitoids intruded subsequently throughout the craton (Moser et al. 2001). The lithosphere became sufficiently rigid by that time to support the development of sedimentary basins (Egglington and Armstrong 2004). This was followed by Ventersdoorp magmatism from 2.8 to 2.6 Ga (Tinker et al. 2002). The NE of the craton was later intruded by the 2.05 Ga old Bushveld complex (Thomas et al. 1993). The periphery of the Kaapvaal craton was reworked in the west between 1.8–2.1 Ga during the Kheis Magondi orogeny (e.g. Alterman and Hölbich 1991) and along its southern margin between 1.2 Ga and 0.9 Ga during the Khibaran orogeny, forming the Namaqua–Natal unit (e.g. Thomas et al. 1993).

Depth and time of melt extraction

Generalities

The dominant rock type of the Kaapvaal cratonic mantle is garnet peridotite. Eclogitic or pyroxenitic assemblages comprise only 2 vol% (Schulze 1989). The melting regime for the precursor rocks to these mantle samples, and their ages, are key pieces of information for the reconstruction of the history and dynamic processes that led to the formation of the Kaapvaal subcratonic mantle. The melting regime may in principal be deduced from bulk rock major and trace element compositions. However, metasomatism is common in subcratonic mantle samples (e.g. Dawson 1984; Keleman et al. 1998) and can disguise the information from the time of partial melting.

Depth of melting – Rare earth elements and Cr_2O_3/Al_2O_3 ratios in peridotites

The long lasting debate about the depth of melting mainly centers around two opposing models: a) deep plume melting followed by isobaric cooling to generate garnet in the residual peridotite (e.g. Boyd 1989; Griffin et al. 1999, 2003; Aulbach 2012) and b) shallow melting followed by subduction and lithosphere thickening to induce garnet growth (e.g. Bulatov et al. 1991; Canil and Wei 1992; Stachel et al. 1998; Pearson and Wittig 2008; Lee and Chin 2014; Wang et al. in press). Limiting parameters as fingerprints of the partial melting process were comprehensively evaluated by Canil (2004), Lee (2006), Lee and Chin (2014), Pearson and Wittig (2008) and Aulbach (2012). They are i) high to very high Mg-values of the peridotites ii) low to very low abundances of mildly incompatible elements like V, Sc and the heavy REE (Rare Earth Elements) and iii) a wide range of bulk rock Cr_2O_3/Al_2O_3 ratios that are reflected in the rocks by a corresponding range of garnet compositions. Consensus exists that the high Mg-values are the result of partial melting of 30 to 40 vol% or more (Bernstein et al. 2007; Pearson and Wittig 2008) and that the low abundances of the mildly incompatible elements exclude the presence of garnet in the residue during the partial melting process.

The origin of the range of Cr_2O_3/Al_2O_3 ratios is the issue. Figure 2 shows an anti-correlation of Yb with Cr_2O_3/Al_2O_3 of peridotites from the Finsch mine that may be exemplary for Kaapvaal peridotite suites. This anti-correlation needs to be

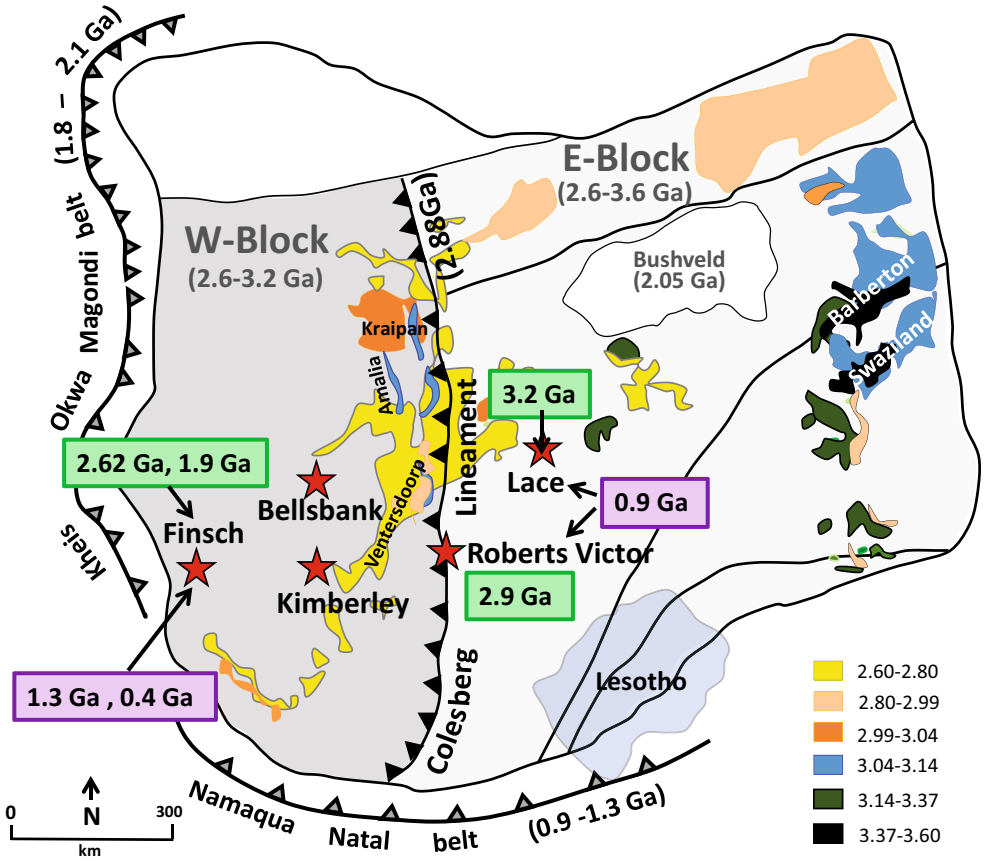

Fig. 1 The main building blocks of the Kaapvaal craton with fields of exposed Paleo- to Neoarchean crystalline basement and volcanic and magmatic rocks and color-coded age divisions after Egglington and Armstrong (2004). Crustal ages range from 2.7 to 3.2 Ga on the W-block and from 2.7 to 3.6 Ga on the E-block. The two blocks collided along the Colesberg lineament 2.88 Ga ago. Ages in green colored boxes are from Lu-Hf and those in violet boxes from Sm-Nd isochrons for metasomatic events at the indicated localities

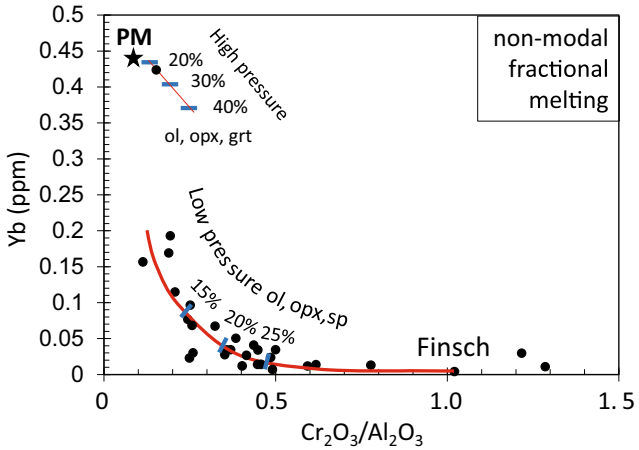

Fig. 2 Covariation of the mildly incompatible element Yb with the Cr/Al ratio in Finsch peridotites. The black dots are bulk rock compositions taken from Gibson et al. (2008) and Lazarov et al. (2012). The red line is an eye fit through the data. It is treated here as representing a partial melting trend. It may, however, be partly overlain by a refertilization process. This would not change the fact that low Yb and high Cr_2O_3/Al_2O_3 ratios are preserved that reflect partial melting at low pressures. The degrees of partial melting (blue bars) are taken for Yb from Lazarov et al. (2012) for fractional, non-modal melting of a pyrolite source in the spinel respectively garnet stability field. The Cr_2O_3/Al_2O_3 ratio for garnet peridotite melting are estimated from the partition coefficients of Canil and Wei (1992)

explained in any partial melting model. The degrees of partial melting given in the figure are taken from Lazarov et al. (2012). They were calculated for Yb for a non-modal fractional melting model. Partial melting in the presence of garnet retains Yb to a large extent in the residuum while any fractional partial melting model depletes Yb very rapidly in the spinel stability field already for smaller degrees of partial melting. In fact, the integrated degrees of partial melting calculated from FeO-MgO relationships after Frey et al. (1985) and Kushiro and Walter (1998) by Lazarov et al. (2012) are higher than for those for Yb at a given Yb content (e.g. for samples where about 20 vol% are calculated for Yb the Fe-MgO relationship yields about 30 vol% and 40 vol% for Fe-O-MgO correspond to 30 vol% for Yb). A non-modal batch melting model for Yb would be in better accord with FeO-MgO.

High pressure melting at >3 GPa by plume subcretion was strongly advocated lately again by Aulbach (2012). The author compared the major element abundances and element ratios of peridotites from most cratons worldwide with bulk rock chemical parameters of model residues. These were modelled from the mineral compositions and modal proportions of low and high pressure melting experiments by Baker and Stolper (1994) and Walter (1998). For the Kaapvaal craton, strongly metasomatized peridotites were excluded from the comparison and distinguished as

orthopyroxene enriched (with too high opx contents for melting residues) or FeO enriched taking the forsterite content of olivine inclusions in diamonds as an anchor. This left a restricted number of samples for the Kaapvaal craton that scatter around high pressure trends of the modelled residues for Cr_2O_3 and Al_2O_3 between 3 and 6 GPa. The Cr_2O_3/Al_2O_3 ratios derived for the residua become high in the model but only for extreme degrees of partial melting (e.g. 1.4 for 50 vol% melting at 3 GPa and about 1 for 70 vol% at 6 GPa). The high values of the model are surprising considering the low Cr_2O_3/Al_2O_3 ratio of the orthopyroxenes in the corresponding experiments; if only olivine and orthopyroxene are left as residual phases in these experiments then the Cr_2O_3/Al_2O_3 ratio of the orthopyroxene is that of the whole rock. The orthopyroxene compositions from the garnet-free 3 to 7 GPa experiments by Walter (1998) are plotted in Fig. 3a. The Cr_2O_3/Al_2O_3 ratio of the orthopyroxenes average at around 0.13, much lower than the modelled values. The reason for the difference is unclear.

Garnet can grow from a garnet-free residue either by isobaric cooling or by an increase of pressure. In our approach to decipher the melting regime, we establish the range of garnet compositions that can grow from a garnet free residue either by exsolution from orthopyroxene by isobaric cooling or via the reaction opx + sp → grt + ol and compare their compositions with those of natural garnets. It has to be kept in mind that the ubiquitous metasomatism in the Kaapvaal mantle is refertilization and reverses the partial melting trend to some extent. Yet it introduces mainly Al over Cr that is usually immobile and can only be transported by saline and alkaline fluids (Klein-BenDavid et al. 2011). The Cr_2O_3/Al_2O_3 bulk rock ratios and those of their garnets will therefore likely be lowered by metasomatism. The range of garnet composition with the higher Cr/Al ratios are therefore significant for deducing the melting regime.

The growth of garnet by exsolution from orthopyroxene during isobaric cooling or with increasing pressure occurs via the reactions

$$2MgSiO_3 + MgAl_2SiO_6 \rightarrow Mg_3Al_2Si_3O_{12} \quad (1)$$

$$2MgSiO_3 + MgCrAlSiO_6 \rightarrow Mg_3CrAlSi_3O_{12} \quad (2)$$

and from orthopyroxene + spinel with increasing pressure via the reactions

$$4MgSiO_3 + MgAl_2O_4 \rightarrow Mg_3Al_2Si_3O_{12} + Mg_2SiO_4 \quad (3)$$

$$4MgSiO_3 + MgCr_2O_4 \rightarrow Mg_3Cr_2Si_3O_{12} + Mg_2SiO_4 \quad (4)$$

Because of the requirement from mildly incompatible element contents that garnet must be absent in the residue (e.g.

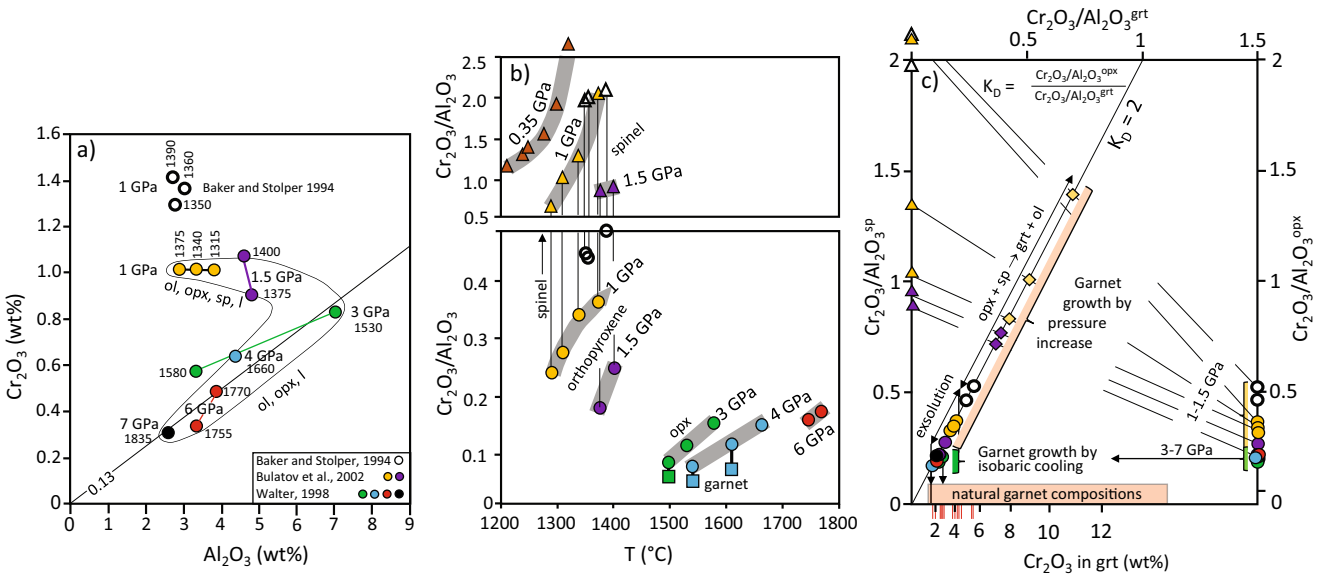

Fig. 3 **a**) Orthopyroxene compositions from peridotite melting experiments by Baker and Stolper (1994), Bulatov et al. (2002) and Walter (1998). Only the compositions from garnet-absent experiments are plotted. **b**) Variations of Cr_2O_3/Al_2O_3 ratios with temperature and pressure of spinel (triangles), orthopyroxene (circles) and garnet (squares) in the melting experiments. Coexisting opx and sp. respectively opx and grt are connected by vertical tie-lines. Olivine is present in all experiments. The brown triangles denote spinel compositions from the experiments by Bulatov et al. (2002) at 0.35 GPa. **c**) The y-axis shows the Cr_2O_3/Al_2O_3 ratios of the experimental spinel on the left and of orthopyroxene on the right. The x-axis denotes the Cr_2O_3/Al_2O_3 ratios of garnet on the top and the corresponding Cr_2O_3-content at the bottom. The composition of garnet grown by exsolution from orthopyroxene can be obtained by projecting the Cr_2O_3/Al_2O_3 ratio of the latter horizontally onto the line for $K_D = 2$. Garnet compositions grown via the reaction opx + sp → grt + ol are obtained from the crossing of the K_D line and the opx-sp tie lines. The pink horizontal bar indicates the range of garnet compositions in natural peridotites. The red bars are the compositions of garnet exsolutions in Kaapvaal orthopyroxenes (Gibson and Mills 2017)

low Yb), only garnet free experiments can be considered in the evaluation of partial melting experiments. Garnet is absent in the high pressure experiments (from 3 GPa onwards) only at very high temperatures where olivine and orthopyroxene coexist with melt. At lower pressures, olivine, orthopyroxene and spinel coexist with melt. Figure 3a shows the compositions of orthopyroxenes from the experiments at 1 GPa by Baker and Stolper (1994), at 1 and 1.5 GPa by Bulatov et al. (2002) and at 3 to 7 GPa by Walter (1998). The orthopyroxenes from the 3–7 GPa experiments have a very similar Cr_2O_3/Al_2O_3 ratio of 0.13 while the low pressure orthopyroxenes have variable Cr_2O_3/Al_2O_3 ratios at higher Cr_2O_3 and similar Al_2O_3 contents. The orthopyroxene from 3 GPa/1530 °C has the highest Al_2O_3 contents (highest garnet potential) at lower Cr_2O_3/Al_2O_3. The Al- and Cr-contents in orthopyroxenes from high pressure (spinel-absent) experiments decrease with increasing temperature because of the increasing amounts of melt in the experiments; the garnet potential accordingly becomes lower. In Fig. 3b the Cr_2O_3/Al_2O_3 ratios of spinel, orthopyroxene and garnet are plotted against temperature. Coexisting phases are connected by vertical tie lines. Orthopyroxene is absent in the lowest pressure experiments of 0.35 GPa by Bulatov et al. (2002) because of the peritectic reaction of orthopyroxene. Spinel and orthopyroxene coexist in the 1 and 1.5 GPa experiments. Garnet and orthopyroxene coexist with olivine and melt at lower temperatures in the higher pressure experiments and orthopyroxene alone at higher temperatures. It is quite apparent that garnets grown from the reaction ol + sp will have higher Cr_2O_3/Al_2O_3 ratios than those grown by exsolution from orthopyroxene alone. It can also be visualized that the Cr_2O_3/Al_2O_3 ratios of orthopyroxenes in Walter's experiments are higher than those of the coexisting garnets (1.3 times higher on average for the three experiments).

Stachel et al. (1998) deduced a value of 2 for the complex $K_D = (Cr_2O_3/Al_2O_3)^{opx}/(Cr_2O_3/Al_2O_3)^{grt}$ from the experiments of Brey et al. (1990). The average K_D is 1.8 for opx-grt pairs from 50 xenoliths from eight localities on the Kaapvaal craton (Hervig et al. 1986) and the average K_D for the couple "garnet exsolutions plus orthopyroxene host" from five Kaapvaal localities is 2 (Gibson and Mills 2017). We use this value of 2 for the K_D in Fig. 3c to estimate garnet compositions that either exsolve from orthopyroxene or grow via the reaction opx + sp → grt + ol. The range of natural garnet compositions in subcratonic peridotites is given there as well and the compositions of garnet exsolutions from Gibson and Mills (2017) are shown as vertical red bars on the x-axis. The composition of garnets exsolving from orthopyroxene or growing by reaction with spinel can be derived either by horizontally projecting the Cr_2O_3/Al_2O_3 ratio of the orthopyroxene onto the line for $K_D = 2$ or from the crossing of the opx-sp tie lines with the K_D line. It may be seen that exsolution from the high pressure (3–7 GPa) orthopyroxenes yields garnets with only 2 to 3 wt% Cr_2O_3. This range would extend to about 6 wt% if the low pressure orthopyroxenes would be considered without their coexisting spinels. The coexistence with spinel up to high temperatures and the growth by the reaction opx + sp is very effective to produce Cr-rich garnets that comprise the range of naturally occurring garnets in peridotites (Fig. 3c). This means, applied to the subcratonic mantle, that residues originated by partial melting at pressures significantly lower than 2 GPa and that the garnets grew by subduction and lithospheric thickening. The major proportion of peridotite underneath the Archean Kaapvaal craton originated by low pressure melting. Plume subcretion and melting at high pressures followed by isobaric cooling is refuted for the majority of samples. Residues of high pressure melting have olivine and orthopyroxene as residual phases with Cr_2O_3/Al_2O_3 ratios around 0.13 that produce only very low-Cr garnets.

Depth of melting – Eu-anomalies in eclogites and the range of $\delta^{18}O$ values

Eclogitic xenoliths comprise a range of rock types from eclogites sensu stricto to garnet pyroxenites to alkremites and grospydites. Their precursor rocks were partial melts of the mantle and cumulates thereof that were altered, devolatized and metamorphosed, metasomatized and partially molten (Jacob 2004). A wide range of $\delta^{18}O$ values with pronounced positive and negative deviations from the mantle value is indicative of seafloor alteration at high and low temperatures (Jacob et al. 2003). They provide a strong argument for a surficial origin of eclogite precursor rocks. The most straightforward argument for an origin at very low pressures are positive Eu-anomalies. They are unique and unequivocal tracers of the low pressure phase plagioclase, betraying that the protoliths of eclogites with this signature were originally low pressure cumulates. Samples with such anomalies occur in almost every eclogite xenolith suite worldwide (Aulbach and Jacob 2016). Two prime examples with pronounced positive Eu- and Sr-anomalies in the clinopyroxenes are shown in Fig. 4a. They belong to a suite of kyanite/corundum eclogites from Bellsbank that are very similar in various geochemical parameters to modern day troctolites from the Atlantic and the Pacific (Shu et al. 2016) and testify the existence of mid ocean-ridge settings and subduction at the time of craton nucleation (see age evaluation below).

Time of melting and depletion

Particularities of age dating of mantle rocks

Ages of a geological process may be derived via radioactive decay systems from isochrons or model ages (schematic

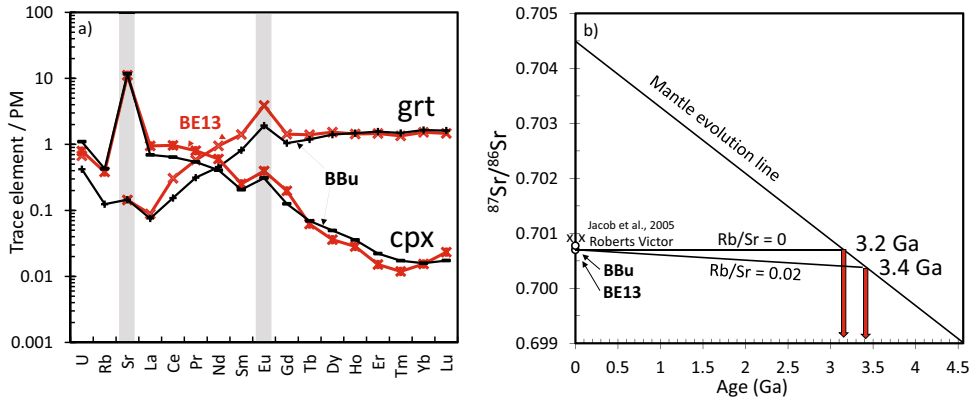

Fig. 4 **a**) Extended REE diagrams of garnets and clinopyroxenes from two corundum eclogites from Bellsbank with pronounced Sr- and Eu-anomalies. **b**) Sr-isotope ratios against the age of the Earth. The low $^{87}Sr/^{86}Sr$ ratios of clinopyroxenes from Roberts Victor are shown in comparison with the two extremely low $^{87}Sr/^{86}Sr$ ratios in clinopyroxenes from the two corundum eclogites from Bellsbank. These values are projected onto the mantle evolution line. These yield minimum model ages of 3.2 to 3.4 Ga (Shu et al. 2016)

diagrams in Fig. S1 a-d). For mantle rocks, the interpretation of the derived ages is not straightforward. Is the "age" of an eclogite that of its precursor rock, metamorphism, metasomatism or partial melting? And for peridotitic residues, is it the age of partial melting or of metasomatism? Bulk rock isochrons would provide the best possibility to date the age of partial melting of peridotites or the age of the precursor rocks for eclogites, although a prerequisite is that xenoliths form a cogenetic group. This may be difficult to prove since the xenoliths stem from a wide depth range. The first, simple barricade, however, lies in the fact that xenoliths are usually contaminated by their host kimberlite. This contamination particularly affects the incompatible elements and with them the Rb-Sr, Sm-Nd and Lu-Hf isotope systems. Therefore, there are almost no isochrons from measured bulk rocks in the literature. Uncontaminated whole rock compositions may be obtained from the composition and modal amounts of clean mineral separates, i.e. of garnet and clinopyroxene. Their isotope ratios combined with their modal abundances would give a reconstructed bulk rock composition. Tie-lines connecting the two minerals in an isochron diagram should yield either the eruption age of the kimberlite or a cooling age.

Early Archean origin of eclogites - unradiogenic Sr isotope ratios in clinopyroxenes

Ages for eclogites from the Kaapvaal craton were estimated for samples from Roberts Victor, Newlands, Lace and Bellsbank. A regression line through bulk rock lead-lead data from Roberts Victor yielded an age around 2.5 Ga (Kramers 1979). A likely age of 2.9 Ga was inferred from lead-lead isotope systematics in clinopyroxenes of eclogites from Lace (Aulbach and Viljoen 2015). Reconstructed bulk rock isochrons for eclogites from Roberts Victor gave about 2.7 Ga for the Sm-Nd and 2.35 Ga for the Lu-Hf isotope system (Jagoutz et al. 1984; Jacob 2004). Menzies et al. (2003) determined the Re-Os isotope systematics of eclogites from Newlands. Lines drawn in an isochron diagram between subsets of the data give an age bracket between 2.9 and 4.1 Ga.

Sr isotope ratios in clinopyroxenes from bimineralic eclogites and garnet pyroxenites have the best potential to preserve old age information. Jacob et al. (2005) and Gonzaga et al. (2010) measured very low $^{87}Sr/^{86}Sr$ ratios in clinopyroxenes of two Roberts Victor eclogites and calculated model ages of around 3 Ga (Fig. 4b). The clinopyroxenes of two eclogites (BE13 and BBu) from Bellsbank have even more unradiogenic $^{87}Sr/^{86}Sr$ ratios of 0.70076 respectively 0.70079 (Fig. 4b), as well as very low Rb/Sr (0.0004 and 0.0006) and high Sr contents (Shu et al. 2016). The low $^{87}Sr/^{86}Sr$ ratios mark the age when Rb was effectively removed from the rocks. A projection onto the mantle evolution line with Rb/Sr = 0 gives a model age of 3.2 Ga (Fig. 4b). This is the absolute minimum age of the eclogites and may mark the time of partial melting of these rocks. The original cumulates should have had at least a 10 times higher Rb/Sr ratio then the present day rocks. This estimate results from the comparison with the Rb/Sr ratios of the gabbroic to troctolitic cumulates from the Pito Deep (Perk et al. 2007). Using a Rb/Sr ratio 0.02 as an approximation for the protolith ratio gives a model age of 3.4 Ga. This may come close to the age of shallow partial melting in the mantle and fractional crystallization within the oceanic crust. These ages are older than the oldest crust formation on the W-block.

Age of partial melting from the Re-Os isotope system

The Re-Os isotope system has the best potential to date melt depletion of mantle peridotites because Os is compatible and Re moderately incompatible during mantle melting (Walker et al. 1989). A large Re-Os data set is now available from the Kaapvaal craton of whole rock and sulfide analyses (Pearson et al. 1995; Carlson et al. 1999; Menzies et al. 1999; Irvine

et al. 2001; Carlson and Moore 2004; Griffin et al. 2004 and Simon et al. (2007). Because there is evidence of recent re-introduction of Re into whole rock samples during the eruptive process only model ages are calculated for each sample and the Re-depletion age T_{RD} is generally preferred. Pearson and Wittig (2008) presented the Kaapvaal T_{RD} ages in a probability density diagram that is reproduced in Fig. 5a. It shows a continuum of ages from about 3.6 Ga to almost 0 with a main peak at about 2.7 Ga. This distribution may be interpreted such that the main time for partial melting was around 2.7 Ga but that partial melting also occurred earlier and later.

If the T_{RD} ages are compared with those of the overlying crust, we find that the major proportion of the crust was formed before 2.9 Ga (the time of collision of the E- and W-block) but that only about 8.5% of the T_{RD} ages are older than 2.9 Ga (Fig. 5a). There seems to be an age mismatch and parts of the mantle and overlying crust may not be genetically related. This apparent mismatch has been discussed before (Carlson et al. 1999; Irvine et al. 2001; Shirey et al. 2004; Griffin et al. 2004) and the tendency of opinions seems to be that the mismatch is due a "diminution" of the T_{RD} ages by metasomatism. T_{RD} model ages are minimum ages by definition because of the assumption that only Re-free, refractory platinum-group minerals are left in the residuum (Lorand et al. 2013) at the high degrees of partial melting. Sulfides are the first to melt in peridotite and any monosulfides or Ni-rich pentlandites now present in the rock must be metasomatic (Pearson et al. 2004). Whole rock analyses of the peridotites therefore contain a mixed information that stems from residual Os-Ir nuggets and reintroduced sulfides with some Re. The sulfides may carry a mix of older and younger information themselves, one from the metasomatic agent and the other from partial reaction with residual platinum-group minerals during metasomatism. Wet-chemical sulfide bulk analyses and in-situ laser ablation analysis of the Re-Os isotopes will therefore yield mixed information as well. Furthermore, depending on the relative spot sizes, a laser may ablate only part of a sulfide. It will give older T_{RD} ages when an Os-Ir nugget is included and younger ages for parts with higher Re. Therefore, some older ages than bulk rock ages can be expected from laser ablation analysis.

The analytical ambiguities and the sulfide-alloy reactions and reintroduction of Re into the system during ancient metasomatism will smear out the bulk rock T_{RD} ages presumably to the wide range as we find it for the Kaapvaal peridotites. But can metasomatism generate a T_{RD} maximum? Or was there an older main period of partial melting and an old T_{RD} maximum is systematically shifted to a younger age by metasomatism? We believe that there is a distinct possibility for either scenario. In Fig. 5b, we show T_{RD} ages of 40 sulfides from eight Finsch peridotites (Griffin et al. 2004) obtained in-situ by LA ICP MS (laser ablation inductively coupled plasma mass spectrometry). The error for each analysis is larger than by conventional analysis because the complete mass overlap of ^{187}Re on ^{187}Os has to be corrected for. Therefore, we have used only the data with low, subchondritic Re/Os ratios where the necessary correction is smaller. The spread and maximum of the T_{RD} values is the same as for the Kaapvaal craton, but there is a larger proportion of older T_{RD} ages. Eight sulfides give values between 3.2 and 3.4 Ga whereas only 3% of the Kaapvaal ages are older than 3.1 Ga. The older ages probably approximate the time of partial melting for the Finsch peridotites more closely than the oldest bulk rock age known from Finsch so far (2.8 Ga; Pearson et al. 1995).

It is also intriguing that there is an age maximum in the sulfide data just like for the bulk rock analyses from the Kaapvaal craton. The sulfide maximum is close to an age of 2.62 Ga as determined by Lazarov et al. (2009) and interpreted by Shu and Brey (2015) as dating the age of carbonatitic metasomatism at Finsch. Sulfide metasomatism may be contemporaneous (because sulfide saturation was reached in the percolating melt) and may have occurred in a peridotite

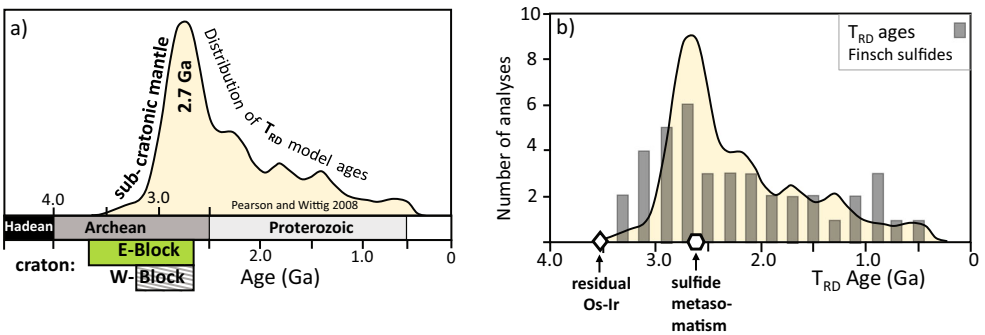

Fig. 5 **a**) A probability density diagram of Re-depletion ages T_{RD} for the lithospheric mantle of the Kaapvaal craton after Pearson and Wittig (2008). It shows a continuum of ages from about 3.6 Ga to almost 0 with a main peak at about 2.7 Ga. The two bars below the age axis indicate the range of crustal ages from the E- and the W-block. **b**) Comparison of 40 selected sulfide T_{RD} ages obtained from eight Finsch peridotites by LA ICP MS (Griffin et al. 2004) with the probability density diagram of Kaapvaal peridotites. Only the data from sulfides with a subchondritic Re/Os ratio were selected. The age of a hypothetical residual Os-Ir alloy is set at 3.6 Ga and sulfide metasomatism is assumed to have occurred at 2.6 Ga, the age of metasomatism at Finsch is taken from Shu et al. (2013)

residuum with 3.6 Ga old Os-Ir alloys (as depicted in Fig. 5b). Using these time constraints and a Platinum Group Element (PGE) + Re composition of a potential metasomatic sulfide (relatively flat chondrite normalized PGE + Re patterns; Luguet et al. 2004) we estimate that the addition of various amounts of sulfide can largely explain the spread of the T_{RD} ages of the Finsch samples. A mean amount of around 0.005 wt% sulfide added to the residue would explain the T_{RD} maximum at around 2.7 Ga. Also, an age maximum of an older main period of partial melting would be shifted to younger ages (to generate a fake maximum for partial melting). Older ages for partial melting are in accord with deductions by Pearson et al. (1995). They concluded in a Re-Os study that the Kaapvaal cratonic mantle had an age of 3.3 to 3.5 Ga. Also, Pearson et al. (2002) found ages of 3.1 Ga for peridotites with highly depleted PGE + Re patterns (depleted Pt, Pd and Re relative to Os and Ir), i.e. for peridotites that probably had not experienced sulfide metasomatism. There is quite a probability that the main period of partial melting for the Kaapvaal craton was before 3.0 Ga.

Time of metasomatism - subcalcic garnets deliver the information

The samples, the metasomatic agent and extent of metasomatism

Defined ages of metasomatism can only be obtained with the Rb-Sr, Sm-Nd and Lu-Hf isotope systems from whole rock isochrons. This is generally impeded by a ubiquitous contamination of the xenoliths by the kimberlite host magma. A solution lies in the isotope analysis of a single mineral grain of sufficient size that contains the major inventory of the incompatible elements. The analysis of such a single grain would represent a whole rock analysis. Subcalcic garnets are suitable candidates (Lazarov et al. 2009). They stem from clinopyroxene-free garnet harzburgites and can be readily identified by their relative CaO and Cr_2O_3 contents (Gurney and Switzer 1972; Sobolev et al. 1973). Since clinopyroxene is absent in their host rock, they are the almost exclusive hosts for many incompatible elements of the bulk rocks. Their analysis therefore corresponds to a whole rock analysis e.g. of the REE, the high field strength elements and of the Sm-Nd and Lu-Hf isotope systems. They are common in heavy mineral concentrates from diamond mines and as inclusions in diamonds.

The grain size needs to be about 3 mm for in situ major and trace element and wet chemical isotope analysis. We collected garnets from the heavy mineral concentrate dumps from the Lace mine on the E-block, the Roberts Victor mine along the Colesberg lineament and the Finsch, Bellsbank and Bultfontein (Boshof road dump) mines on the W-block. The garnet compositions are plotted in Fig. 6a in a Cr_2O_3-CaO diagram. They all lie in the cpx-free, harzburgitic field. The field of all garnet compositions from heavy mineral concentrates and inclusions in diamonds from the Finsch mine is shown for comparison. Depths of origin were estimated by projecting the averaged temperatures of the Ni in garnet thermometers of Griffin et al. (1989) and Canil (1999) onto a conductive geothermal gradient corresponding to 40 mW/m^2 (Chapman and Pollack 1977) (Fig. 6b). The garnets from the Lace mine stem from depths of 140–185 km, those from Roberts Victor from 125 to 175 km, the Finsch samples come from 150 to 180 km, Bellsbank from 90 to 120 km and those from Kimberley from 110 to 150 km.

The degree of metasomatic overprint must have been small, too small to be detected by the identification method of Griffin et al. (1999). The majority of the garnets plot in their "depleted peridotite field" in a Y versus Zr diagram (not shown). We traced the nature of the metasomatic agent with more sensitive elements for metasomatism following Rudnick et al. (1992) and Yaxley et al. (1991). They found that high, superchondritic Zr/Hf ratios and low, subchondritic Ti/Eu ratios are indicators of carbonatitic metasomatism. The vast majority of the garnets have superchondritic Zr/Hf and subchondritic Ti/Eu ratios indicating that they equilibrated with a carbonatitic melt (Shu and Brey 2015). A subgroup has only slightly elevated Zr/Hf ratios and lowered Ti/Eu ratios and the garnets probably interacted with a kimberlitic melt.

The garnets were divided into 2 or 3 groups at each locality by the latter authors depending on the relative abundances of the middle and heavy REE and their Zr and Hf systematics. An example is shown in Fig. 7a,b for subcalcic garnets from Roberts Victor. The REE patterns commonly show sinusoidal Primitive Mantle (PM)-normalized patterns, others have light REE depleted patterns with flat middle to heavy REE and with Lu and Yb contents higher than the sinusoidal garnets. Sinusoidal and non-sinusoidal subcalcic garnets are randomly distributed within the mantle column (Fig. 7c). In this figure we use the Ni-content of the garnets as a proxy of the depth of derivation. The type of REE patterns are expressed as $(Eu/Gd)_{C1}$ ratios.

The range of patterns is very similar to that found in subcalcic garnet inclusions in diamonds (Stachel and Harris 2008). This concurrence allows the conclusion that metasomatism and crystallization of diamonds are joint processes (Stachel and Harris 1997).

We modelled metasomatism by carbonatitic or kimberlitic melts as an open system process with multiple sources of the metasomatizing agent within the mantle column, with partial equilibration of the percolating melt with the depleted mantle by a process of dissolution and re-precipitation and with a residual melt moving on. High degrees of melting at low pressures generate ol-opx-sp residues with very low light REE and low heavy REE that are almost exclusively included in a pre-metasomatic garnet after high pressure

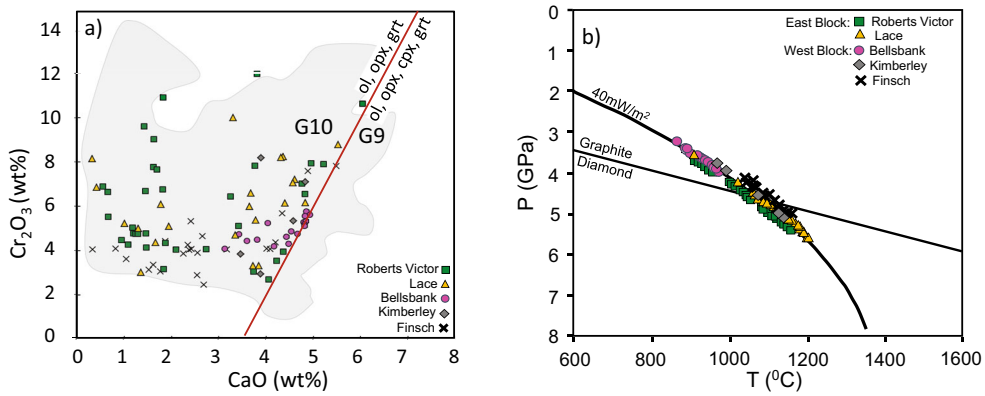

Fig. 6 **a**) The compositions of subcalcic garnets from our studies. The compositional field of garnets from Finsch heavy mineral concentrates (Gurney and Switzer 1972; Grutter et al. 2006) and inclusions in diamonds (Gurney et al. 1979) are shown for comparison. The red line is the dividing line between cpx-present and absent lithologies. **b**) The depth of derivation of the garnets was obtained by projecting the averages of Ni-temperatures calculated from Griffin et al. (1989) and Canil (1999) onto a geothermal gradient corresponding to a heat flow of 40 mW/m^2

metamorphism (Fig. 7a,b). Carbonatitic and kimberlitic agents have highly fractionated REE patterns with high light REE and low HREE contents (Fig. 7a,b). Our model calculations show that the interaction of 1–3 vol% of a carbonatitic agent (relative to the amount of garnet) is sufficient to produce the group RV1 and RV2 garnets. The patterns of the RV3 garnets can be generated by the interaction of about 10 vol% of a kimberlitic melt.

The elements Lu and Hf are relatively more compatible than Sm and Nd (see their relative positions in Fig. 7). Only very small degrees of metasomatism would not affect the Lu-Hf system and only then, it would be possible to determine the age of partial melting with this system. The Sm-Nd system is immediately affected by metasomatism and its age could be determined by isochrons. More intense metasomatism would also affect the Lu-Hf system and then, both system give the age information on metasomatism. Any subsequent metasomatic event will affect especially Sm-Nd again and the age information becomes blurred.

Age of metasomatism

The isotope ratios of the Sm-Nd and Lu-Hf systems in the subcalcic garnets were determined by wet chemistry and MC ICP MS (multi collector inductively coupled plasma mass spectrometry). The values are shown in Fig. 8 as εHf versus εNd values. There are four quadrants in this diagram, one for partial melting and three for various degrees of metasomatism. The intensity of metasomatism of premetasomatic garnets with these elements and their isotopes determines whether one can obtain age information on the partial melting process or on metasomatism. The values of residues of partial melting

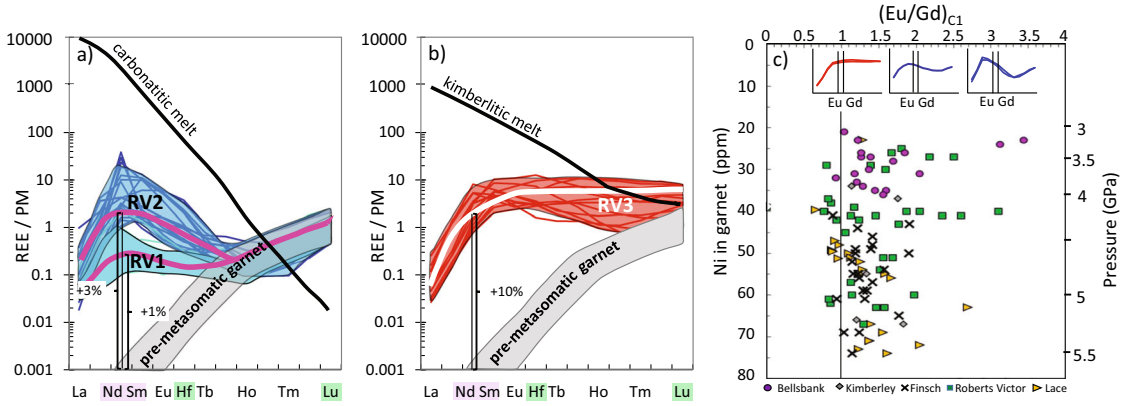

Fig. 7 The garnets from the various localities can be subdivided into two to three groups according to their REE patterns as shown here for Roberts Victor garnets as an example (Shu and Brey 2015). The patterns are composites of a pre-metasomatic garnet and of a highly REE fractionated metasomatic agent that reacted with garnet during percolation through the mantle. It was shown by Shu and Brey (2015) that it should be **a**) a carbonatitic agent for RV 1 and 2 garnets and **b**) a kimberlitic agent for RV3 garnets. The compositions of the model carbonatitic and kimberlitic metasomatic agents and the degrees of metasomatism in vol% are taken from Shu and Brey (2015). **c**) Distribution of the variously metasomatized types of subcalcic garnets in the lithospheric mantle column. Ni in garnet is taken as a proxy for depth based on the calibrations of Griffin et al. (1989) and Canil (1999)

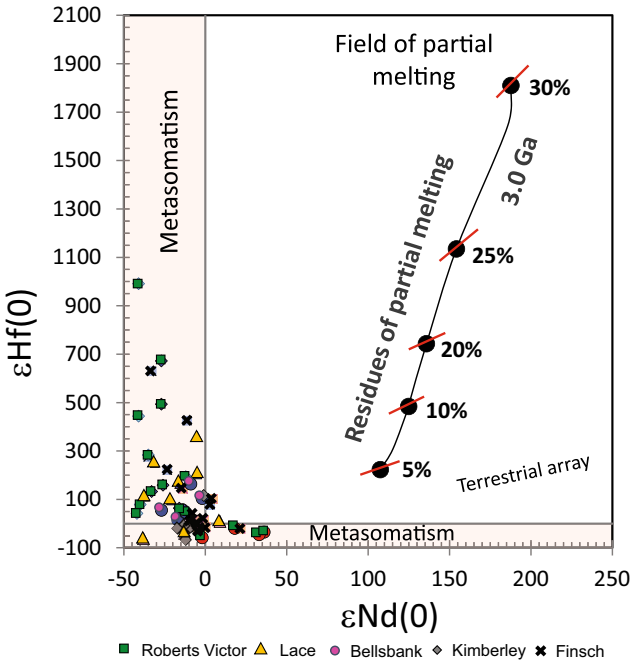

Fig. 8 A diagram of εHf versus εNd for subcalcic garnets after Shu and Brey (2015). Garnets from non-metasomatized residues should plot in the upper right quadrant like the residues calculated for partial melting in the spinel stability field 3 Ga ago. All analysed garnets plot in the fields for metasomatism. Isochron ages for metasomatism can be obtained from these data. The very negative εNd and εHf values correspond to the initials of the metasomatizing agent that overwhelmed the isotopic composition of the substrate

would plot into the upper right quadrant along trends of increasing degrees of partial melting. A trend calculated for modal batch melting 3 Ga ago in the spinel stability field is shown in Fig. 8. None of the subcalcic garnets plot along this trend nor into the quadrant because metasomatism apparently has overwhelmed the age information for partial melting in both isotope systems.

When the data for the various garnet groups are plotted into isochron diagrams, linear arrays are formed for the Lu-Hf system (Fig. 9 a,b,c,d; after Lazarov et al. 2009 and Shu et al. 2013) that should date the time of metasomatism. The age of 2.94 ± 0.05 Ga at Roberts Victor coincides with the time of collision of the E- and W-block along the Colesberg lineament (Fig. 1). The 2.62 ± 0.11 Ga age from Finsch overlaps with Ventersdoorp magmatism and the 1.9 ± 0.19 Ga age with that of the Kheis Magondi belt. An age of 3.2 ± 0.5 Ga arises from the correlation for Lace that is from around the time when the various segments of the E-block amalgamated. The Sm-Nd isotope system also yields correlations but with larger errors. The ages of these correlations (Lazarov et al. 2009; Shu et al. 2013) are shown in Fig. 1. The age of 0.9 Ga at Lace and Roberts Victor may be correlated with the Namaqua Natal belt, for the other two ages from Finsch there are no obvious counterparts within or around the rims of the craton.

The ancient character of the metasomatic agent – a crustal link?

Metasomatism decouples the Lu-Hf and Sm-Nd isotope systems, and εHf and εNd values can become independently positive or negative (Fig. 8). Nevertheless, high to very high εHf values still keep the memory of an ancient melting event. The extremely negative εNd and εHf values are the signatures of the metasomatic agent assuming complete overprinting of the protolith isotopes. This will occur most readily in strongly depleted protoliths and easier for Nd than for Hf (Fig. 7). The agent was carbonatitic to kimberlitic (see above) and must have been derived from a very old source in the lithosphere that already had very low Sm/Nd and Lu/Hf ratios which prevented the growth of ^{143}Nd and ^{176}Hf. The high LREE contents and high Nd/Sm ratios of the carbonatitic agent overwhelmed the strongly depleted peridotite and imparted their old signature with εNd < −40. Similar negative εNd values were found in Cr-diopsides from various Kaapvaal localities (Menzies and Murthy 1980) and even more negative values in subcalcic garnets from the Newland kimberlite on the West Kaapvaal craton (Klein-BenDavid and Pearson 2009; D.G. Pearson informed us that the samples quoted as being from Ekati in that paper actually stem from Newlands). Highly negative values were also measured in pooled garnet inclusions in diamonds from Kimberley and Finsch (Richardson et al. 1984). The model ages of the subcalcic garnets and of the inclusions in diamonds are around 3.4 Ga (Fig. 10a). Analogous to Nd, present day εHf values of subcalcic garnets can be extremely negative down to −65. Model ages up to 3.6 Ga are obtained (Fig. 10b). Again, the very negative εHf values require the derivation of the metasomatic agent from an old component in the mantle with a crustal signature.

An additional characteristic of subcalcic garnets with very low εNd values (xenocrysts and inclusions in diamond) are highly radiogenic ^{87}Sr/^{86}Sr ratios up to 0. 732 that are not supported by correspondingly high Rb/Sr ratios (Richardson et al. 1984; Jacob et al. 1998; Klein-BenDavid and Pearson 2009). The high ^{87}Sr/^{86}Sr ratios must have been imparted by a metasomatic agent. Fluids or melts causing such signatures cannot come from the convecting asthenosphere (Klein-BenDavid and Pearson 2009) because their source must have low Sm/Nd and high Rb/Sr ratios. The source may have been subducted carbonated pelites or hybrid products of carbonated pelite-peridotite interaction (Foley 2010; Grassi and Schmidt 2011; Bulatov et al. 2014; Rapp et al. 2017) or from seafloor altered basalts.

The cooling of the mantle

The geothermal gradient at the time of kimberlite eruption can be determined by thermobarometry on xenoliths and

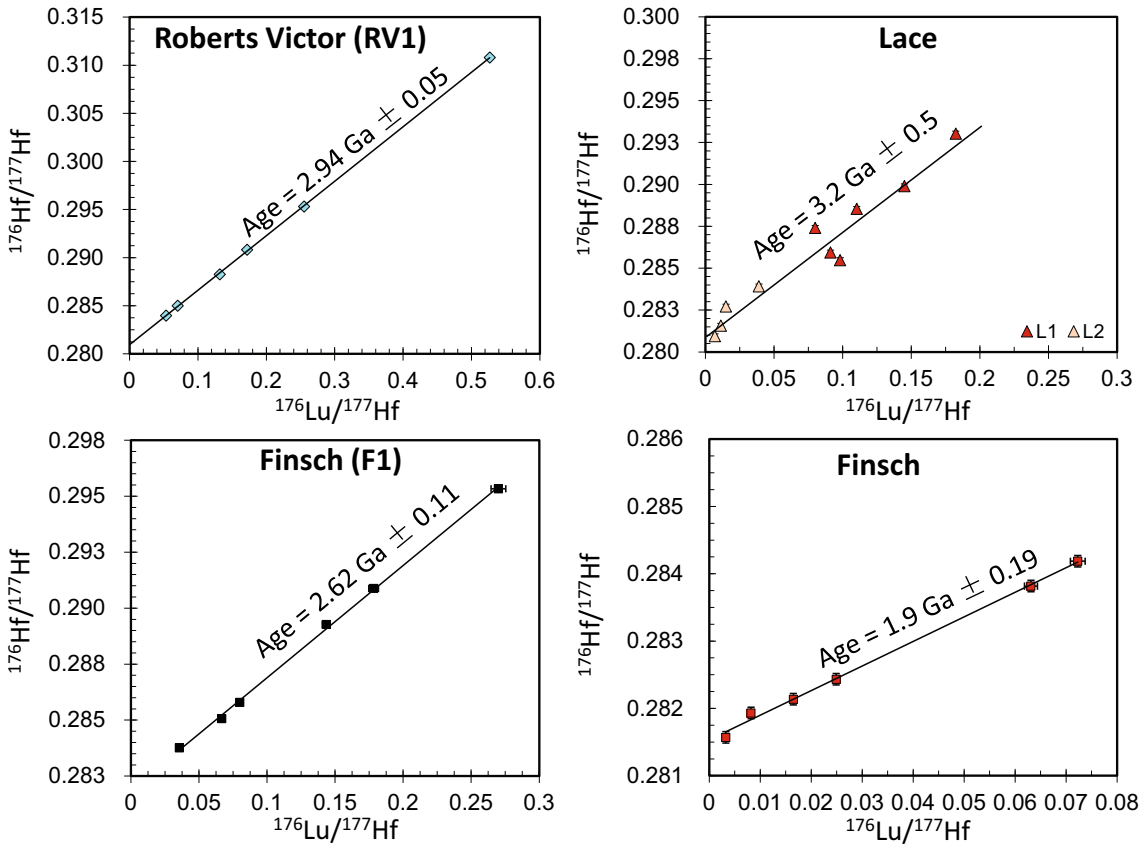

Fig. 9 The Lu-Hf isotope system yields isochrons that date the age of metasomatism at the various localities. The isochrons give 2.9 Ga at Roberts Victor, 3.2 Ga at Lace and 2.64 and 1.9 Ga at Finsch. Diagrams after Lazarov et al. (2009) and Shu et al. (2013)

xenocrysts. A compilation of P,T data from Kaapvaal xenoliths by Bell et al. (2003) shows that the data plot around an average geothermal gradient corresponding to a heat flow of about 40 mW/m^2 with thermal perturbations at the base of the lithosphere (Fig. 11). These authors used the formulations for the two pyroxene thermometer and the Al-in-opx barometer as calibrated by Brey and Köhler (1990). A comparison shows that very similar results are obtained with the formulations of Nimis and Grütter (2010).

No tectonomagmatic event has affected the Kaapvaal craton since 2.6 Ga except for the intrusion of the Bushveld complex 2.05 Ga ago, and Michaut and Jaupart (2007) suggested that the lithospheric mantle had reached thermal equilibrium by the end of the Archean. A stable geothermal gradient had developed in a subcratonic mantle almost devoid of heat-producing radioactive elements with a crust enriched in heat-producing elements above and the asthenosphere underneath. They also suggested that the mantle most likely cooled since then with a rate that is a function of the reduction of the heat flow from the convecting mantle, the diminishing heat production from the decay of U, Th and K in the crust and heat dissipation into space. Heat loss by erosional uplift is negligible because

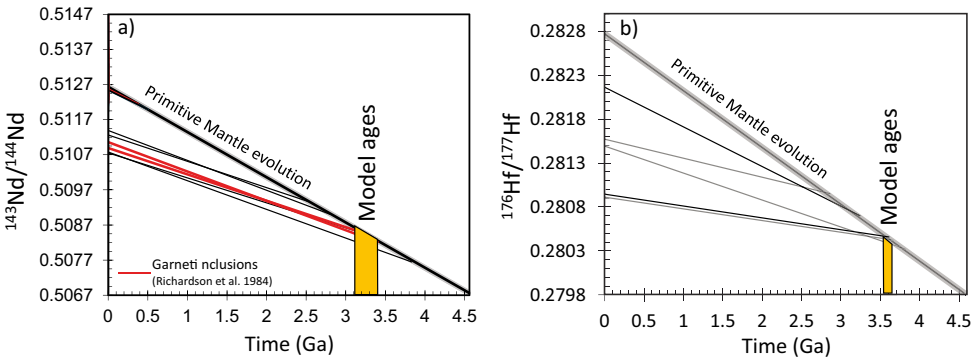

Fig. 10 **a**) Model ages for the subcalcic garnets with the most negative εNd values and from garnet inclusions in diamonds. **b**) Model ages for the subcalcic garnets with the most negative εHf values. Both diagrams are simplified from Shu and Brey (2015)

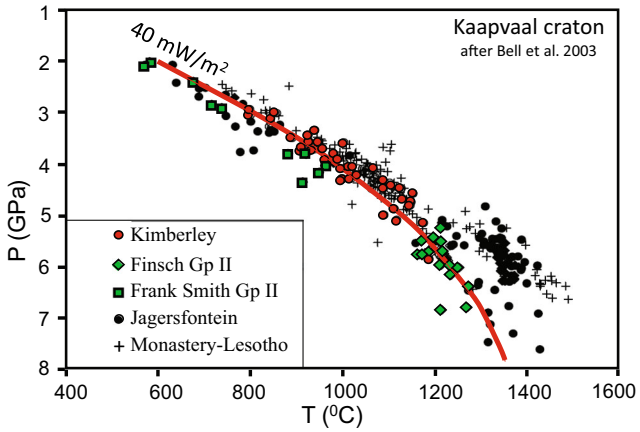

Fig. 11 The geothermal gradient of the Kaapvaal craton at the time of kimberlite eruption after Bell et al. (2003)

Archean greenstone belts are almost non-metamorphic and the crustal thickness did not change significantly since 3 Ga (Galer and Mezger 1998). Each increment in the mantle remained at practically the same depth since its stabilization (Fig. 12). Increments are indicated in Fig. 12 as layers of eclogites that do not change their depth level with time.

Cooling in a stationary mantle has consequences for the interpretation of data from radioactive isotope systems. Isotherms that move downwards with time (Fig. 12) will cross the closure temperature of the isotope systems. If the closure temperatures are different for different isotope systems, the isotopic exchange between coexisting phases will stop at different times for the same mantle increment and the radioactive clock will start for one system and only later for that with the lower closure temperature. If there is no other disturbance grt-cpx tie lines should therefore give the eruption age of the kimberlite if ambient temperatures were above the closure temperatures or cooling ages that increase with the decreasing temperature of last equilibration.

The chemical compositions of minerals adjust to changing physical conditions by volume and grain boundary diffusion. Grain boundary diffusion is strongly enhanced by a melt or a fluid phase and volume diffusion by hydrogen in nominally anhydrous minerals like garnet and clinopyroxene. Diffusion of an element further depends on temperature, on its ionic size and its charge. Smaller, divalent cations like Fe^{2+} and Mg^{2+} diffuse faster than the significantly larger trivalent REE and the tetravalent Hf^{4+} (e.g. Ganguly and Tirone 1999; Dutch and Hand 2010). Diffusion therefore stops earlier for the tri- and tetravalent cations during cooling than for divalent cations. In other words, the closure temperatures of geochronological systems are reached earlier than the temperatures when the

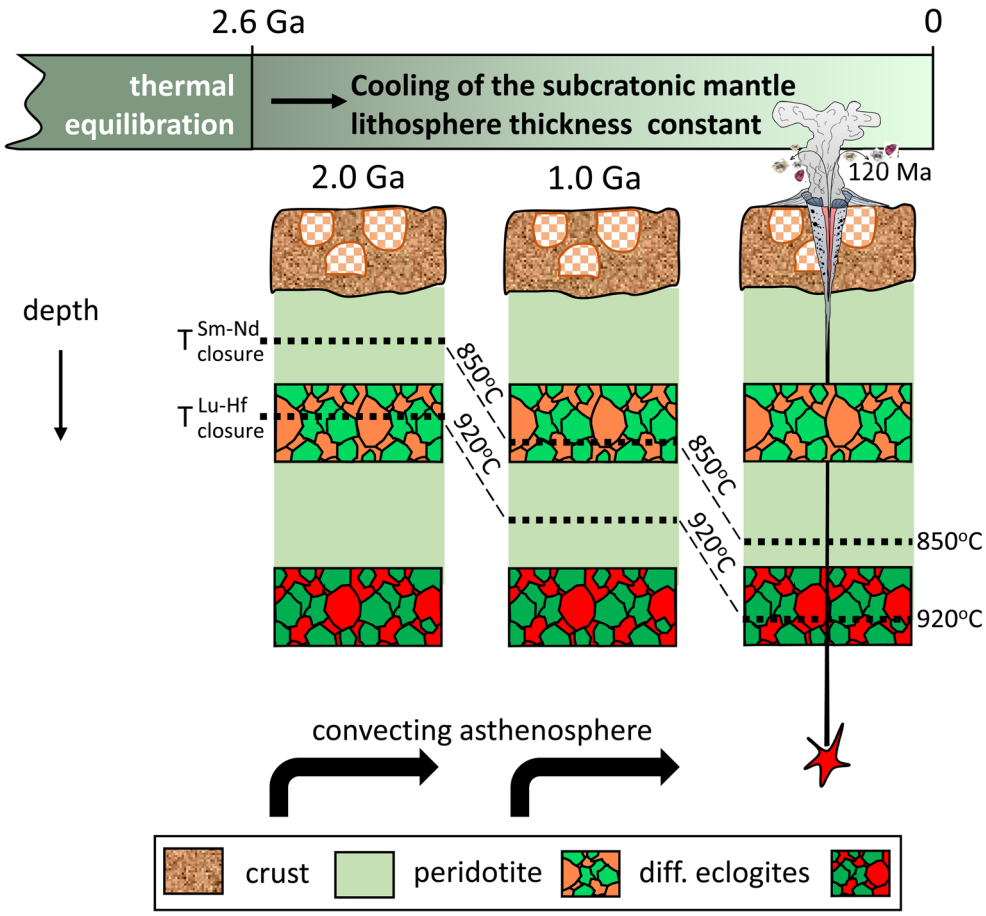

Fig. 12 Shift of isotherms with time to increasingly greater depths in a cooling mantle (schematic). Individual increments in the mantle (shown schematically as different types of eclogites) remain stationary over time. Isotopic exchange between minerals stops at the closure temperatures of the respective isotope systems. A mantle portion maybe just at the closure temperature for Lu-Hf 2 Ga ago. The radioactive clock begins to tick while the isotopic exchange for Sm-Nd continues. The same mantle portion will be at the closure temperature for Sm-Nd one Ga later and this clock starts as well. Kimberlite eruptions bring samples to the surface from great depths that are in isotopic equilibrium and samples from shallower depths from below the closure temperatures. The cooling rate of the mantle can be estimated from the age difference of the closure temperatures and the differences of the two ages in individual samples

ionic exchange of divalent cations stops as well. Calculated temperatures of last equilibration based on the exchange of Fe and Mg are therefore still meaningful when temperatures already had dropped below the closure temperatures for the Sm-Nd and Lu-Hf isotope systems.

Shu et al. (2014) plotted the temperatures of last equilibration in the mantle (calculated from Krogh 1988) of eclogites and garnet pyroxenites from Bellsbank, Roberts Victor and a few other samples from the Kaapvaal craton (and from Diavik in Canada) against the ages of the grt-cpx tie-lines. They found an envelope around the data with two limiting boundaries. One is a negative correlation at low temperatures of increasing age with decreasing temperature and the second is a horizontal line with kimberlite eruption age. These lines are reproduced in Fig. 13a. The two lines intersect at around 920 °C for the Lu-Hf and around 850 °C for Sm-Nd system. The intersects were taken as the closure temperatures of the isotope systems. The difference between the closure temperatures is 70 °C.

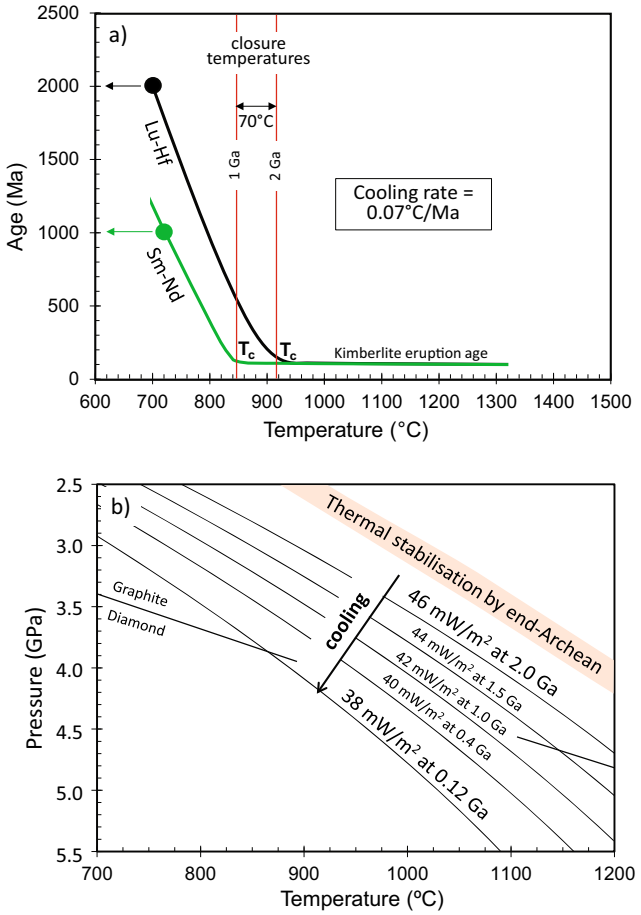

Fig. 13 **a**) A diagram of grt-cpx ages versus temperature of last equilibration in the mantle. Ages increase with decreasing temperatures below the closure temperature and correspond to kimberlite eruption age at higher temperatures. The lines are reproduced from Shu et al. (2014). A cooling rate of around 0.07 °C/Ma can be estimated from the differences of the low temperature limbs. **b**) Because the mantle increments are stationary since the end of the Archean the data from the low temperature limbs can be plotted into a P,T diagram (Shu et al. 2014). The superposition of geothermal gradients on the data shows that the mantle cooled from a geothermal gradient of 46 mW/m^2 2 Ga ago to 38 mW/m^2 at the time of kimberlite eruption

The Lu-Hf and Sm-Nd ages of the lowest temperature sample of the whole data set are plotted in Fig. 13a. The grt-cpx tie-lines give ages of about 2 Ga for Lu-Hf and 1 Ga for Sm-Nd. This means that this eclogitic piece of the mantle from a depth of about 90 km cooled by about 70 °C over a period of 1 Ga. The differences for individual samples of the cooling ages along the low temperature limbs of the two isotope systems combined with the closure temperatures can be used to deduce the cooling of the subcratonic mantle from the early Proterozoic until today (Fig. 13b). Shu et al. (2014) found that the subcratonic mantle cooled since 2 Ga from a geothermal gradient of 46 mW/m^2 to the present day geothermal gradient with a rate of around 0.07 °C/Ma. Such a value is in agreement with estimates that were based on various geophysical and geological constraints, heat production by radioactive elements and diffusivity of radiogenic elements. The cooling of the Kaapvaal subcratonic mantle may show up from a comparison of geothermal gradients derived for a peridotite suite of the 90 Ma northern Lesotho kimberlites with that of the 1180 Ma Premier mine (see Fig. 2 in Pearson 1999). The Premier peridotites yield a hotter geothermal gradient than the Lesotho peridotites.

A synopsis

As pointed out in the Introduction, a major issue over the last decades was the depth of melting and melt separation for the subcratonic mantle. We demonstrated above from of Cr_2O_3/Al_2O_3 relationships that this occurred at very shallow depths. Partial melting may have occurred at mid ocean ridges followed by subduction similar to modern Earth or by upwelling in a hotter Archean environment followed by down drag due to eclogitisation at the base of oceanic plateaus as another kind of subduction (Fig. 14). Lithospheric thickening may have occurred by slab stacking as suggested by Helmstaedt and Schulze (1989), down-welling (Lee and Chin 2014) or lateral compression and gravitational self-thickening (Wang et al. in press). Herzberg and Rudnick (2012) suggested that a very thick lithosphere was directly created due to a high Archean heat flow. In whatever model subduction will create thermal and chemical inhomogeneities (Fig. 14) that strive towards equilibration. It will occur by liberation of fluids, partial melting, melt-rock interaction and heat transfer. The thermal and chemical adjustment leads to metasomatism and crustal growth and loss of dense residua (from eclogite melting) that may sink into the deep mantle. This would explain the paucity of eclogites in the Kaapvaal mantle. Subduction and lithosphere thickening may have occurred at defined times so that metasomatism also occurred periodically.

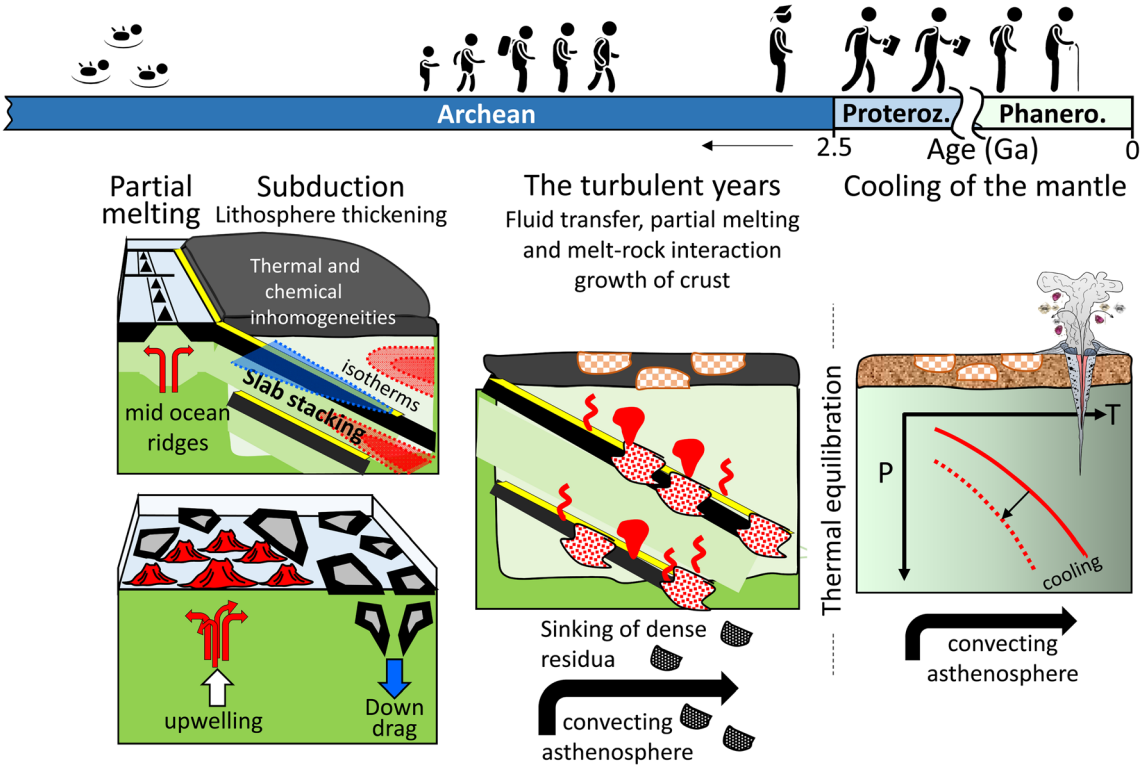

Fig. 14 The birth, growth and ageing of the subcratonic mantle in a picture story. The Kaapvaal craton consists of a number of fragments so that it can be expected that a number of various mantle nuclei were created by partial melting as well. Two models are shown for adiabatic upwelling and melt separation at low pressures followed by subduction or vertical down drag. Subduction underneath an oceanic plateau corresponds to a model for the origin of cratonic nuclei by Nair and Chacko (2008). Lithosphere thickening may occur by slab stacking (Helmstaedt and Schulze 1989) or by a two-stage thickening process (Wang et al. in press) or variants. Any kind of a subduction process leads to strong temperature and chemical inhomogeneities. These strive towards equilibration by fluid transfer, partial melting and melt-rock interactions between the various lithologies like subducted sediments, fresh and altered ocean floor and depleted peridotite. This leads to growth and modification of the continental crust. Dense eclogite residua of these processes may sink into the deep mantle. This may explain the paucity of eclogitic material in the subcratonic mantle. The turbulent years end by the establishment of a stable geothermal gradient (Michaut and Jaupart 2007) probably by the end of the Archean followed by cooling up to now

The partial melting and differentiation processes led to an almost complete partitioning of the incompatible, radioactive and heat-producing elements U, Th and K into the crust and the lithospheric mantle was probably almost entirely depleted (e.g. Michaut and Jaupart 2007). These authors suggested that these turbulent years were terminated near the end of the Archean by the establishment of a stable geothermal gradient in the mantle between the overlying crust and the hot asthenosphere underneath. We determined that the mantle cooed since then with a rate of about 0.07 °C/Ma.

A number of studies have investigated the similarities and differences of the age of processes in the crust and underlying mantle of the Kaapvaal craton (e.g. Helmstaedt and Schulze 1989; Griffin et al. 2004; Pearson and Wittig 2008; Shu and Brey 2015). The available age information for various processes in crust and mantle of the Kaapvaal lithosphere is summarized in Fig. 15. The most pronounced discrepancy is a mismatch between the ages from crust and mantle before 3.1 Ga. The T_{RD} model ages for the whole Kaapvaal craton span a range from 3.6 Ga to zero but only about 3% are older than 3.1 Ga. The cratonic nuclei of the E-block were mainly built before that time. Oldest crustal ages are 3.6 Ga and the amalgamation of the various segments probably occurred at around 3.2 Ga ago (Schoene et al. 2008). Metasomatism in the mantle may have accompanied the amalgamation as indicated by the 3.2 Ga isochron (admittedly with a large error of 0.5 Ga) from the Lu-Hf isotope system.

The small number of old T_{RD} ages are shared by peridotite samples both from the E-and the W-block but oldest crustal ages from the W-block are about 3.1 Ga, i.e., the mantle or parts of it underneath this block are older than the overlying crust. Furthermore, a number of processes besides partial melting occurred in the mantle that are older than any crustal age. Richardson et al. (1984) reported that diamonds were formed underneath Finsch and Kimberley at 3.2 and 3.3 Ga. These ages are Nd model ages and not an absolute proof that diamond grew at that time; however, a number of good reasons support that conclusion. Independent of that uncertainty in interpretation, these old model ages and very negative εNd values (−36) bring the information that an old crustal

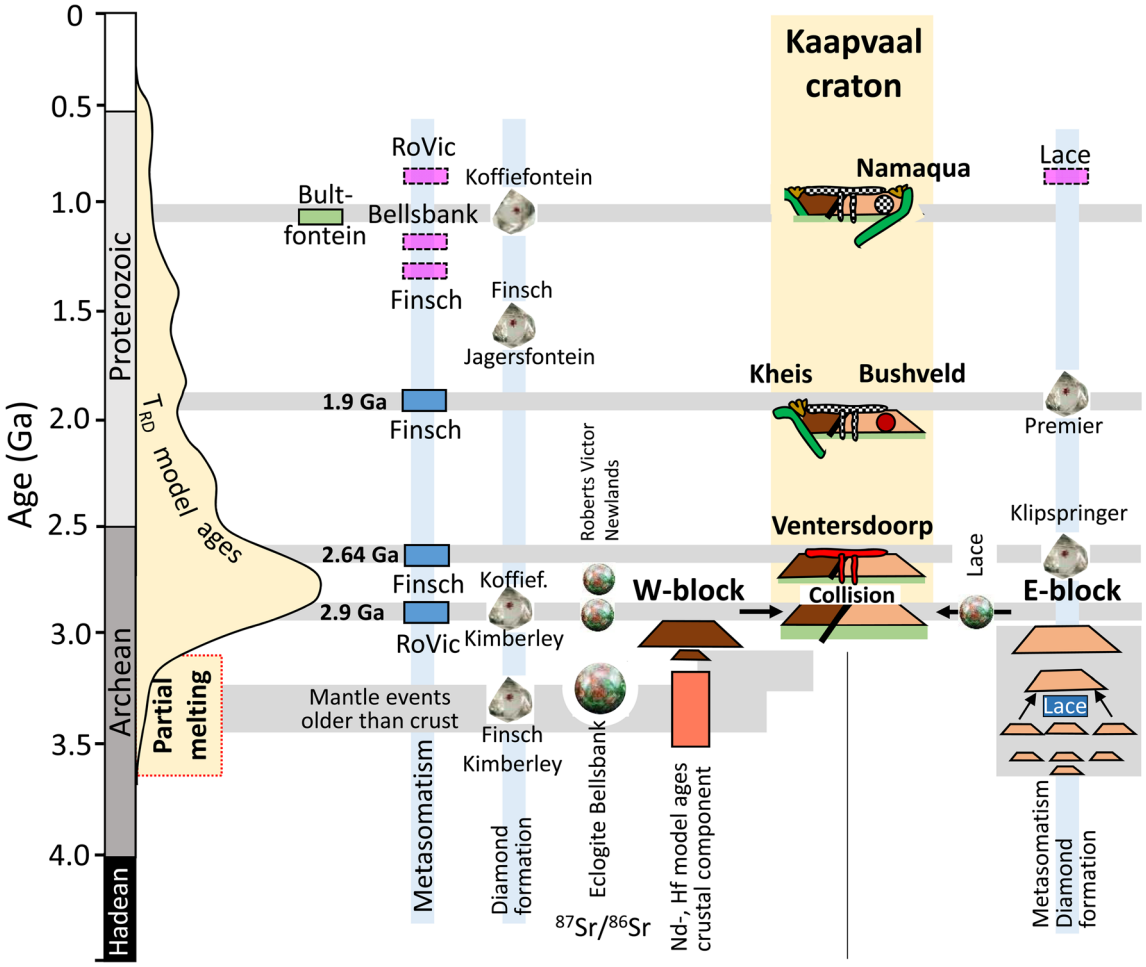

Fig. 15 The history of the development of the Kaapvaal craton and its underlying mantle. The time axis is shown on the left as a vertical bar together with the compilation of T_{RD} ages after Pearson and Wittig (2008). The red-framed box between 3.6 and 3.1 Ga represents our interpretation of the age of the main period of partial melting. The growth of the crust is indicated by trapezoids (dark brown for the W- and light brown for the E- block). Their development is separate until their collision around 2.9 Ga ago. The period of Ventersdoorp magmatism from 2.8 to 2.6 Ga is indicated by two red vertical and a horizontal bar. The green slab is the symbol for the Kheis Magondy orogeny between 1.8 to 2.1 Ga at the west periphery of the craton and the red ball for the intrusion of the Bushveld complex 2.05 Ga ago. This was followed by the Khibaran orogeny between 1.2 and 0.9 Ga that formed the Namaqua-Natal unit in the southern periphery of the craton. Mantle events are shown separately for the E- and the W-block. The range of Nd- and Hf-model ages of crustal components underneath the W-block is shown by a pink bar. Isochron ages for metasomatism are indicated by horizontal bars in blue for the Lu-Hf and in lilac for the Sm-Nd isotope system. The light green bar indicates a phlogopite Ar-Ar age from Bultfontein. The eclogite balls indicate eclogite formation ages and the diamond with a garnet inclusion (picture from SH Richardson, University of Cape Town) ages of diamond formation. References for the ages are given in the text. The names attached to the symbols are those of diamond mines

component already existed in the mantle at that time. The same information is obtained from the most negative εNd (−41) and εHf (−65) values of the subcalcic garnet xenocrysts (Fig. 10). Such time-integrated isotopic systematics can only stem from a very old (early Archean) crustal component subducted into the mantle. Subduction before the onset of crust formation on the W-block is proven by the presence of eclogites from Bellsbank with extremely low $^{87}Sr/^{86}Sr$ ratios (Fig. 4b). Their precursor rocks were likely generated as olplagioclase cumulates (troctolites) at very low pressures, subducted and partially melted (Shu et al. 2016). The low $^{87}Sr/^{86}Sr$ ratios require a minimum age for these processes of 3.2 Ga. A memory of very old partial melting events probably in the Paleoarchean (red-framed box in Fig. 15) may be preserved only rarely by the oldest T_{RD} ages of the peridotites and their sulfides. Most ages were overprinted by metasomatic processes in the Meso- to Neoarchean.

The resemblance of the major and trace elements compositions of the kyanite/corundum eclogites to modern day troctolites from the Atlantic and Pacific (Shu et al. 2016) implies that the melting of the mantle occurred at shallow depths. The peridotites themselves carry a signature that they were residues from low pressure melting and were metamorphosed during subduction. The vast majority of their garnets contain 4 to 12 wt% Cr_2O_3, with some reaching up to 20 wt% in the extreme in occurrences. As discussed above Cr-rich residues

can only originate by partial melting as long as spinel is a residual phase. Cr-rich garnets grow in these residues by subduction via the reaction opx + sp → grt + ol. The low pressures of melting have to be reconciled with the high degrees of melting required by the high to very Mg-values of 92–94 of the peridotites.

In the Phanerozoic, oceanic plateaus are probably the products of high degrees of partial melting and the result of hot mantle plumes. In the Archean, thick oceanic crust and depleted mantle may form in a mid-ocean ridge environment and upwelling mantle by high degrees of melting and low final melting pressures because of high ambient mantle potential temperatures (Herzberg and Rudnick 2012). These authors imply mantle potential temperatures around 1600 °C, beginning of melting at 3–6 GPa and final melting pressures at 1–3 GPa resulting in 25 to 45 vol% partial melting. Such a model is in accord with the requirements from the Cr_2O_3/Al_2O_3 ratios for residues from low pressure melting. Herzberg and Rudnick (2012) disposed of the surplus eclogite generated in such a model by partial melting to generate the crust and by foundering of the residues. Subsequent rising of buoyant harzburgite diapirs and the assembly of cratonic nuclei substantially modify the sublithospheric mantle in their model.

Pearson and Wittig (2008) and reevaluation by Pearson et al. (in press) also favor low pressure melting of less than 3 GPa. They express, however, difficulties in reaching high degrees of melting at relevant ambient mantle potential temperatures during anhydrous melting. They find, based on the modelling of Iwamori et al. (1995) and modelling of experimental data summarized by Herzberg (2004) that the melt production rate at lower pressures is less than at higher pressures. An increased melt production at low pressures could be brought about by the presence of water during melting in Archean subduction zones. These residues are re-enriched in orthopyroxene to variable extent by rising siliceous melts stemming from orthopyroxene breakdown at deeper levels. The lithospheric roots are formed by subduction stacking. Such a model would fulfill the requirements for low-P melting imposed by Cr_2O_3/Al_2O_3 ratios.

An interesting model is that of Nair and Chacko (2008) for the origin of continental crust and the initiation of intra-oceanic subduction. They suggest that intra oceanic subduction originates in the Archean due to gravitational instabilities produced by compositional and density contrasts between converging oceanic plateau and normal oceanic lithosphere. This is shown schematically in Fig. 14). Subduction of oceanic lithosphere (sediments, basalts, gabbroic cumulates) occurs into the 'hot' mantle residuum below newly formed oceanic plateau crust (Fig. 14). The final pressures of melting and degrees of melting vary in such a model depending on whether it occurs for oceanic plateau or midoceanic ridge settings. Pressures are, however, always low to very low. Temperature differences between the "hot" mantle and the subducted material are more pronounced than today that will lead to more rigorous reactions between the various lithologies (see below). If lithospheric thickening is generated by slab stacking (Helmstaedt and Schulze 1989) it produces a more complex thermal structure and multiple chemical layering.

Thermal and chemical inhomogeneities are inherent in all the above models because they all contain a subduction component. These will strive towards equilibration by the liberation of fluids from sediments and altered oceanic crust, fluid-rock and melt-rock interaction, possibly further melting in depleted peridotite and by heat exchange (Fig. 14). Orthopyroxene, clinopyroxene and garnet will be reintroduced to some extent into depleted peridotite from the neighboring lithologies as a kind of auto-metasomatism and dense eclogitic residua of these processes will sink and disappear in the asthenospheric mantle. This process should increase the buoyancy of the bulk of the lithospheric mantle as a whole.

Tectonomagmatism in the crust seems to occur in time intervals in the Archean. If its cause is due to processes in the mantle and subduction into the mantle it implies that subduction, partial melting, metasomatism, formation of diamonds etc. also occurs at defined time intervals. We have identified discrete metasomatic events by Lu-Hf isochrons of subcalcic garnets from Lace, Roberts Victor and Finsch (Fig. 9 and blue boxes in Fig. 15) and obtained indications for further metasomatic events from the Sm-Nd isotope system (Lazarov et al. 2009; Shu and Brey 2015; and purple boxes in Fig. 15). The event at Lace at 3.2 Ga corresponds to the amalgamation of the cratonic nuclei of the E-block. The 2.9 Ga metasomatic event determined at Roberts Victor marks a major event for the craton. It corresponds to the collision of the E- and W-blocks (Schmitz et al. 2004), the time of formation of diamonds at Koffiefontein and Kimberley (Aulbach et al. 2009) and probably eclogite formation at Roberts Victor (Jacob et al. 2003) and Lace (Aulbach and Viljoen 2015). The 2.62 Ga old metasomatic event at Finsch coincides with the final stages of Ventersdoorp magmatism (2.8–2.6 Ga; Tinker et al. 2002) and probably marks the final stage of cratonization of the Kaapvaal craton. Later events are probably induced by processes along the rifted margins of the craton like the 1.9 Ga event at Finsch by the Kheis Magondi belt (Alterman and Hölbich 1991). The Bushveld intrusion at 2.05 Ga (Thomas et al. 1993) may have induced diamond formation underneath the Premier mine around this time. The Ar-Ar-ages from metasomatic phlogopites between 1 and 1.2 Ga (Hopp et al. 2008) from Bultfontein are an almost 1:1 match to the Namaqua-Natal orogenesis around the southern and south-western margin of the Kaapvaal craton (Thomas et al. 1993). The ages from around that time from Roberts Victor, Bellsbank and Lace indicated by the Sm-Nd isotope system (purple boxes) may be related to this event.

We have identified carbonatitic to kimberlitic melts as the main agents for metasomatism in cpx-free garnet harzburgites from diagnostic trace element ratios such as Ti/Eu and Zr/Hf (Shu and Brey 2015). Substantial overlap of the Ti/Eu and Zr/Hf ratios in subcalcic garnets and garnet inclusions in diamonds corroborate previous findings that mantle metasomatism and the growth of diamonds are connected processes. Shu and Brey (2015) envisaged a process of the interaction of a carbonatitic melt with depleted garnet harzburgite by dissolution and regrowth of the constituent minerals and the growth of diamonds by redox reactions. Model calculations show that only small amounts of a carbonatite melt in the range of 0.3 to 3 vol% are needed to generate the range of sinusoidal REE patterns in the garnets from harzburgites and the inclusions in diamonds. The main growth period for diamonds may coincide with this period of consolidation that is characterized by thermal and chemical inhomogeneities. The P,T conditions of growth derived from inclusions in diamonds scatter in between a range of geothermal gradients (from 36 to 42 mW/m^2; see summary by Stachel and Harris 2008). This may express that temperatures in the mantle may have been quite variable in similar depth intervals and diamonds may have grown in similar depths but at a range of temperatures.

Subsequent to these turbulent years, probably around 2.6 Ga ago, thermal consolidation generated a stable thermal structure between a heat producing upper crustal lid and the convective asthenosphere (Michaut and Jaupart 2007). Figure 13b shows that a conductive geothermal gradient of about 46 mW/m^2 was established by 2.0 Ga (Shu et al. 2014). They found that the subcratonic mantle cools since that time with a rate of about 0.07 °C/Ma.

Acknowledgements We would like to thank Vadim Bulatov, Axel Gerdes, Andrei Girnis, Jeff Harris, Jan Heliosch, Heidi Höfer, Franz Kneissl, Linda Marco, Anna Neumann, Graham Pearson, Jock Robey, Janina Schastok, Hans-Michael Seitz, Thomas Stachel, Stefan Weyer and Armin Zeh for their continuous help in the field and laboratory and fruitful discussions over the years. We thank an anonymous reviewer and Graham Pearson for very many helpful and positive suggestions. The research was supported by the Deutsche Forschungsgemeinschaft, a scholarship from the China Scholarship Council and the Canada Excellence Research Chairs program.

References

Alterman W, Hölbich IW (1991) Structural history of the southwestern corner of the Kaapvaal craton and the adjacent Namaqua realm: new observations and reappraisal. Precambrian Res 52:133–166

Aulbach S (2012) Craton nucleation and formation of thick lithospheric roots. Lithos 149:16–30

Aulbach S, Jacob DE (2016) Major- and trace-elements in cratonic mantle eclogites and pyroxenites reveal heterogeneous sources and metamorphic processing of low-pressure protoliths. Lithos 262: 586–605

Aulbach S, Shirey SB, Stachel T, Creighton S, Muehlenbachs K, Harris JW (2009) Diamond formation episodes at the southern margin of the Kaapvaal Craton: Re-Os systematics of sulfide inclusions from the Jagersfontein Mine. Contrib Mineral Petrol 157(4):525–540

Aulbach S, Viljoen KS (2015) Eclogite xenoliths from the Lace kimberlite, Kaapvaal craton: from convecting mantle source to palaeo-ocean floor and back. Earth Planet Sc Lett 431:274–286

Baker MB, Stolper EM (1994) Determining the composition of high-pressure mantle melts using diamond aggregates. Geochim Cosmochim Ac 58:2811–2827

Bell DR, Schmitz MD, Janney PE (2003) Mesozoic thermal evolution of the southern African mantle lithosphere. Lithos 71(2–4):273–287

Bernstein S, Keleman PB, Hanghøj K (2007) Consistent olivine Mg# in cratonic mantle reflects Archean mantle melting to the exhaustion of orthopyroxene. Geology 35(5):459–462

Boyd FR (1989) Compositional distinction between oceanic and cratonic lithosphere. Earth Planet Sc Lett 96:15–26

Brey GP, Köhler T (1990) Geothermobarometry in 4-phase lherzolites II. New thermobarometers, and practical assessment of existing thermometers. J Petrol 31(6):1353–1378

Brey GP, Köhler T, Nickel KG (1990) Geothermobarometry in four-phase lherzolites. I. Experimental results from 10 to 60 kb. J Petrol 31:1313–1352

Bulatov V, Brey GP, Foley SF (1991) Origin of low-Ca, high-Cr garnets by recrystallization of low-pressure harzburgites, 5th Int Kimberlite Conf. Araxa, Extended Abstracts, Companhia de Pesquisa de Recursos Minerais Special Publication 91:29–31

Bulatov V, Girnis AV, Brey GP (2002) Experimental melting of a modally heterogeneous mantle. Mineral Petrol 75:131–152

Bulatov VK, Brey GP, Girnis AV, Gerdes A, Hoefer HE (2014) Carbonated sediment–peridotite interaction and melting at 7.5–12 GPa. Lithos 200-201:368–385

Canil D (1999) The Ni-in garnet geothermometer: calibration at natural abundances. Contrib Miner Petr136:240–246

Canil D (2004) Mildly incompatible elements in peridotites and the origins of mantle lithosphere. Lithos 77:375–393

Canil D, Wei K (1992) Constraints on the origin of mantle-derived low Ca garnets. Contrib Mineral Petrol 109:421–430

Carlson RW, Moore RO (2004) Age of the Eastern Kaapvaal mantle: Re–Os isotope data for peridotite xenoliths from the monastery mine. S Afr J Geol 107:81–90

Carlson RW, Pearson DG, Boyd FR, Shirey SB, Irvine G, Menzies AH, Gurney JJ (1999) Re–Os systematics of lithospheric peridotites: implications for lithosphere formation and preservation. In: Gurney JJ, Gurney JL, Pascoe MD, Richardson SH (eds) Proceedings of the VIIth International Kimberlite Conference. Red Roof Designs, Cape Town, pp 99–108

Chapman DS, Pollack HN (1977) Regional geotherms and lithospheric thicknesses. Geology 5:265–268

Dawson JB (1984). Contrasting types of mantle metasomatism? In: Kornprobst J (ed) Kimberlites II; the mantle and crust–mantle relationships. Elsevier, Amsterdam, pp 289–294

Dutch R, Hand M (2010) Retention of Sm–Nd isotopic ages in garnets subjected to high-grade thermal reworking: implications for diffusion rates of major and rare earth elements and the Sm–Nd closure temperature in garnet. Contrib Mineral Petrol 159(1):93–112

Egglington BM, Armstrong RA (2004) The Kaapvaal Craton and adjacent orogens, southern Africa: a geochronological database and overview of the geological development of the craton. S Afr J Geol 107:13–32

Foley SF (2010) A reappraisal of redox melting in the Earth's mantle as a function of tectonic setting and time. J Petrol 52(7–8):1363–1391

Frey FA, John SC, Stockman HW (1985) The Ronda high temperature peridotite: geochemistry and petrogenesis. Geochim Cosmochim Ac 49:2469–2491

Galer SJG, Mezger K (1998) Metamorphism, denudation and sea level in the Archean and cooling of the Earth. Precambrian Res 92:389–412

Ganguly J, Tirone M (1999) Diffusion closure temperature and age of a mineral with arbitrary extent of diffusion: theoretical formulation and applications. Earth Planet Sc Lett 170:131–140

Gibson SA, Malarkey J, Day JA (2008) Melt depletion and enrichment beneath the western Kaapvaal Craton: evidence from Finsch peridotite xenoliths. J Petrol 49:1817–1852

Gibson SA, Mills S (2017) On the nature and origin of garnet in highly-refractory Archean lithospheric mantle: constraints from garnet exsolved in Kaapvaal craton orthopyroxenes. Mineral Mag 81(4): 781–809

Gonzaga RG, Menzies MA, Thirlwall MF, Jacob DE, LeRoex A (2010) Eclogites and garnet pyroxenites: Problems resolving provenance using Lu-Hf, Sm-Nd and Rb-Sr isotope systems. J Petrol 51:513–535

Grassi D, Schmidt MW (2011) Melting of carbonated pelites at 8–13 GPa: generating K-rich carbonatites for mantle metasomatism. Contrib Mineral Petrol 162:169–191

Griffin WL, Cousens DR, Ryan CG, Sie SH, Suter GF (1989) Ni in chrome pyrope garnets–a new geothermometer. Contrib Mineral Petrol 103:199–202

Griffin WL, Graham S, O'Reilly SY, Pearson NJ (2004) Lithosphere evolution beneath the Kaapvaal Craton: Re–Os systematics of sulfides in mantle-derived peridotites. Chem Geol 208:89–118

Griffin WL, O'Reilly SY, Natapov LM, Ryan CG (2003) The evolution of lithospheric mantle beneath the Kalahari Craton and its margins. Lithos 71:215–241

Griffin WL, O'Reilly SY, Afonso JC, Begg GC (2009) The composition and evolution of lithospheric mantle: a re-evaluation and its tectonic implications. J Petrol 50:1185–1204

Griffin WL, Shee SR, Ryan CG, Win TT, Wyatt BA (1999) Harzburgite to lherzolite and back again: metasomatic processes in ultramafic xenoliths from the Wesselton kimberlite, Kimberley, South Africa. Contrib Mineral Petrol 134:232–250

Grutter H, Latti D, Menzies A (2006) Cr-saturation arrays in concentrate garnet compositions from kimberlite and their use in mantle barometry. J Petrol 47:801–820

Gurney JJ, Harris JW, Rickard RS (1979) Silicate and oxide inclusions in diamonds from the Finsch kimberlite pipe. Proceedings of the 2nd International Kimberlite Conference, vol 1, pp 1–14

Gurney JJ, Switzer GS (1972) The discovery of garnets closely related to diamonds in the Finsch pipe, South Africa. Contrib Mineral Petrol 39:103–116

Helmstaedt H. and Schulze DJ (1989) Southern African kimberlites and their mantle sample; implication for Archean tectonics and lithosphere evolution. In: Ross J (ed) Kimberlites and related rocks, vol 1 Geol Soc Australia Special Publication 14:358–368

Hervig RL, Smith JB, Dawson JB (1986) Lherzolite xenoliths in kimberlites and basalts: petrogenetic and crystallographic significance of some minor and trace elements in olivine, pyroxenes, garnet and spinel. T Roy Soc Edin-Earth 77:181–201

Herzberg C (2004) Geodynamic information in peridotite petrology. J Petrol 45:2507–2530

Herzberg C, Rudnick R (2012) Formation of cratonic lithosphere: an integrated thermal and petrological model. Lithos 149:4–15

Hopp J, Trieloff M, Brey GP, Woodland AB, Simon NSC, Wijbrans JR, Siebel W, Reitter E (2008) $^{40}Ar/^{39}Ar$-ages of phlogopite in mantle xenoliths from South African kimberlites: evidence for metasomatic mantle impregnation during the Kibaran orogenic cycle. Lithos 106(3–4):351–364

Irvine GJ, Pearson DG, Carlson RW (2001) Lithospheric mantle evolution in the Kaapvaal craton: a Re–Os isotope study of peridotite xenoliths from Lesotho kimberlites. Geophys Res Lett 28:2505–2508

Iwamori H, McKenzie D, Takahashi E (1995) Melt generation by isentropic mantle upwelling. Earth Planet Sc Lett 134:253–266

Jacob DE (2004) Nature and origin of eclogite xenoliths from kimberlites. Lithos 77:295–316

Jacob DE, Bizimis M, Salters VJM (2005) Lu/Hf and geochemical systematics of recycled ancient oceanic crust: evidence from Roberts Victor eclogites. Contrib Mineral Petrol 148(6):707–720

Jacob DE, Jagoutz E, Sobolev NV (1998) Neodymium and strontium isotopic measurements on single subcalcic garnet grains from Yakutian kimberlites. Neues Jb Mineral Abh 172(2–3):357–379

Jacob DE, Schmickler B, Schulze DJ (2003) Trace element geochemistry of coesite-bearing eclogites from the Roberts Victor kimberlite, Kaapvaal craton. Lithos 71:337–351

Jagoutz E, Dawson JB, Hoernes S, Spettel B, Wänke H (1984) Anorthositic oceanic crust in the Archean Earth. 15th Lunar and Planetary Science Conference, pp 395–396 (abstract)

Jordan TH (1988) Structure and formation of the continental tectonosphere. In: Menzies MA and cox KG eds oceanic and continental lithosphere: similarities and differences. Oxford university Press, Oxford. J Petrol Spec Vol 1:11–37

Keleman PB, Hart SR, Bernstein S (1998) Silica enrichment in the continental upper mantle via melt/rock reaction. Earth Planet Sc Lett 164(1–2):387–406

Klein-BenDavid O, Pearson DG (2009) Origins of subcalcic garnets and their relation to diamond forming fluids - case studies from Ekati (NWT-Canada) and Murowa (Zimbabwe). Geochim Cosmochim Ac 73:837–855

Klein-BenDavid O, Pettke T, Kessel R (2011) Chromium mobility in hydrous fluids at upper mantle conditions. Lithos 125:122–130

Kramers JD (1979) Lead, uranium, strontium, potassium and rubidium in inclusion-bearing diamonds and mantle-derived xenoliths from Southern Africa. Earth Planet Sc Lett 42:58–70

Krogh EJ (1988) The garnet-clinopyroxene Fe-Mg geothermometer -a reinterpretation of existing experimental data. Contrib Mineral Petrol 99:44–48

Kushiro I, Walter MJ (1998) Mg–Fe partitioning between olivine and mafic-ultramafic melts. Geophys Res Lett 25:2337–2340

Lazarov M, Brey GB, Weyer S (2009) Time steps of depletion and enrichment in the Kaapvaal craton as recorded by subcalcic garnets from Finsch (SA). Earth Planet Sc Lett 27:1–10

Lazarov M, Brey GP, Weyer S (2012) Evolution of the South African mantle—a case study of garnet peridotites from the Finsch diamond mine (Kaapvaal craton); part 2: multiple depletion and re-enrichment processes. Lithos 154:210–224

Lee CT (2006) Geochemical/petrologic constraints on the origin of cratonic mantle, Archean geodynamics and environments. In: Benn K, Mareschal JC, Condie LC (eds) Archean geodynamics and environments. Geophysical Monograph Series vol 164, pp 89–114

Lee C-TA, Chin EJ (2014) Calculating melting temperatures and pressures of peridotite protoliths: implications for the origin of cratonic mantle. Earth Planet Sc Lett 403:273–286

Lorand J-P, Luguet A, Alard O (2013) Platinum-group element systematics and petrogenetic processing of the continental upper mantle: a review. Lithos 164–167:2–21

Luguet A, Lorand J-P, Alard O, Cottin J-Y (2004) A multi-technique study of platinum group element systematic in some Ligurian ophiolitic peridotites. Chem Geol 208:175–194

Menzies AH, Carlson RW, Shirey SB, Gurney JJ (2003) Re–Os systematics of diamond-bearing eclogites from the Newlands kimberlite. Lithos 71:323–336

Menzies AH, Shirey SB, Carlson RW, Gurney JJ (1999) Re–Os systematics of Newlands peridotite xenoliths: implications for diamond and lithosphere formation. In: Gurney JJ, Gurney JL, Pascoe MD, Richardson SH (eds) Proceedings of the 7th International Kimberlite Conference. Red Roof Design, Cape Town, pp 566–583

Menzies M, Murthy VR (1980) Enriched mantle: Nd and Sr isotopes in diopsides from kimberlite nodules. Nature 283(5748):634–636

Michaut C, Jaupart C (2007) Secular cooling and thermal structure of continental lithosphere. Earth Planet Sc Lett 257:83–96

Moser DE, Flowers RM, Hart RJ (2001) Birth of the Kaapvaal tectosphere 3.08 billion years ago. Science 291:465–468

Nair R, Chacko T (2008) Role of oceanic plateaus in the initiation of subduction and origin of continental crust. Geology 36:583–586

Nimis P, Grütter H (2010) Internally consistent geothermometers for garnet peridotites and pyroxenites. Contrib Mineral Petrol 159(3):411–427

O'Reilly SY, Griffin WL (2013) Mantle Metasomatism. In: Harlov D, Austrheim A (eds) Metasomatism and the chemical transformation of rock. Lecture Notes in Earth System Sciences. Springer, Berlin Heidelberg, pp 471–533

Pearson DG (1999) The age of continental roots. Lithos 48:171–194

Pearson DG, Carlson RW, Shirey SB, Boyd FR, Nixon PH (1995) Stabilisation of Archean lithospheric mantle: a Re–Os isotope study of peridotite xenoliths from the Kaapvaal Craton. Earth Planet Sc Lett 134:341–357

Pearson DG, Irvine GJ, Carlson RW, Kopylova MG, Ionov DA (2002) The development of lithospheric mantle keels beneath the earliest continents: time constraints using PGE and Re-Os isotope systematics. In: Fowler CMR (ed) The early Earth: physical, chemical and biological development. Geol Soc SP 199:65–90

Pearson DG, Irvine GJ, Ionov DA, Boyd FR, Dreibus GE (2004) Re-Os isotope systematics and Platinum Group Element fractionation during mantle melt extraction: a study of massif and xenolith peridotite suites. Chem Geol 208:29–59

Pearson DG, Liu J, Smith CB, Mather KA, Krebs MY, Bulanova GP, Kobussen A (in press) Characteristics and origin of the mantle root beneath the Murowa diamond mine: implications for craton and diamond formation. Society of Economic Geologists Special Publication

Pearson DG, Wittig N (2008) Formation of Archaean continental lithosphere and its diamonds: the root of the problem. J Geol Soc Lond 165:895–914

Perk NW, Coogan LA, Karson JA, Klein EM, Hanna HD (2007) Petrology and geochemistry of primitive lower oceanic crust from Pito Deep: implications for the accretion of the lower crust at the southern East Pacific rise. Contrib Mineral Petrol 154:575–590

Peslier AH, Woodland AB, Bell DR, Lazarov M (2010) Olivine water contents in the continental lithosphere and the longevity of cratons. Nature 467:78–81

Rapp RP, Timmerman S, Lowczak J, Jaques AL (2017) Metasomatism of Cratonic Lithosphere by Hydrous, Silica-rich, Fluids Derived from Recycled Sediment: Experimental Insights at 5–7 GPa. 11th International Kimberlite Conference, Extended Abstract 11IKC-4640

Richardson S, Gurney J, Erlank A, Harris J (1984) Origin of diamonds in old enriched mantle. Nature 310:198–202

Rudnick RL, McDonough WF, Chappell BW (1992) Carbonatite metasomatism in the northern Tanzanian mantle – petrographic and geochemical characteristics. Earth Planet Sc Lett 114:463–475

Schmitz MD, Bowring SA, de Wit MJ, Gartz V (2004) Subduction and terrane collision stabilize the western Kaapvaal craton tectosphere 2.9 billion years ago. Earth Planet Sc Lett 222:363–376

Schoene B, de Wit MJ, Bowring SA (2008) Mesoarchean assembly and stabilization of the eastern Kaapvaal craton: a structural-thermochronological perspective. Tectonics 27(5): TC5010

Schulze DJ (1989) Constraints on the abundance of eclogite in the upper mantle. J Geophys Res 94:4205–4212

Shirey SB, Richardson SH, Harris JW (2004) Integrated model of diamond formation and craton evolution. Lithos 77:923–944

Shu Q, Brey GP (2015) Ancient mantle metasomatism recorded in subcalcic garnet xenocrysts: temporal links between mantle metasomatism, diamond growth and crustal tectonomagmatism. Earth Planet Sc Lett 418:27–39

Shu Q, Brey GP, Gerdes A, Höfer HE (2013) Geochronological and geochemical constraints on the formation and evolution of the mantle underneath the Kaapvaal craton: Lu–Hf and Sm–Nd systematics of subcalcic garnets from highly depleted peridotites. Geochim Cosmochim Ac 113:1–20

Shu Q, Brey GP, Gerdes A, Höfer HE (2014) Mantle eclogites and garnet pyroxenites– the meaning of two-point isochrons, Sm–Nd and Lu–Hf closure temperatures and the cooling of the subcratonic mantle. Earth Planet Sc Lett 389:143–154

Shu Q, Brey GP, Hoefer HE, Zhao Z, Pearson DG (2016) Kyanite/corundum eclogites from the Kaapvaal Craton: subducted troctolites and layered gabbros from the mid- to early Archean. Contrib Mineral Petrol 171:11

Simon NSC, Carlson RW, Pearson DG, Davies GR (2007) The origin and evolution of the Kaapvaal cratonic lithospheric mantle. J Petrol 48: 589–625

Sobolev NV, Lavrent'ev YG, Pokhilenko NP, Usova LV (1973) Chrome-rich garnets from kimberlites of Yakutia and their parageneses. Contrib Mineral Petrol 40:39–52

Stachel T, Harris JW (1997) Diamond precipitation and mantle metasomatism–evidence from the trace element chemistry of silicate inclusions in diamonds from Akwatia, Ghana. Contrib Mineral Petrol 129(2):143–154

Stachel T, Harris JW (2008) The origin of cratonic diamonds – constraints from min-eral inclusions. Ore Geol Rev 34:5–32

Stachel T, Viljoen KS, Brey GP, Harris JW (1998) Metasomatic processes in lherzolitic and harzburgitic domains of diamondiferous lithospheric mantle: REE in garnets from xenoliths and inclusions in diamonds. Earth Planet Sc Lett 159:1–12

Thomas RJ, von Veh MW, McCourt S (1993) The tectonic evolution of southern Africa: an overview. J Afr Earth Sci 16:5–24

Tinker J, De Wit MJ, Grotzinger JP (2002) Seismic stratigraphic constraints on Neoarchean - Paleoproterozoic evolution of the western margin of the Kaapvaal craton, South Africa. S Afr J Geol 105:107–134

Walker RJ, Carlson RW, Shirey SB, Boyd FR (1989) Os, Sr, Nd, and Pb isotope systematics of southern African peridotite xenoliths: implications for the chemical evolution of subcontinental mantle. Geochim Cosmochim Ac 53:1583–1595

Walter MJ (1998) Melting of garnet peridotite and the origin of komatiite and depleted lithosphere. J Petrol 39(1):29–60

Wang H, van Hunen J, Pearson DG (in press) Making Archean cratonic roots by lateral compression: a two-stage thickening and stabilization model. Tectonophysics

Yaxley GM, Crawford AJ, Green DH (1991) Evidence for carbonatite metasomatism in spinel peridotite xenoliths from western Victoria, Australia. Earth Planet Sc Lett 107:305–317